

FINAL DRAFT: 10 FEB 92

Volume 15

**THE FOUR-DIMENSIONAL
FIRE INDUCED TRANSMITTANCE AND TURBULENCE EFFECTS MODEL
FITTE**

Dorothy Bruce

**US Army Atmospheric Sciences Laboratory
White Sands Missile Range, New Mexico 88002-5501**

February 1992

Contents

Introduction	5
1.2 Availability	6
1.2.1 Mailing Address	6
1.2.2 Phone and Electronic Mail	6
Background	7
2.1 Conceptual Overview of FITTE	8
2.2 The Physical Models	8
2.2.1 The Fire and Fire Plume Models	8
2.2.1.1 The Time-averaged Fire	8
2.2.1.2 The Time-averaged Fire Plume	10
2.2.1.3 Time-Averaged Plume Effluent and Temperature Distribution Functions	13
2.2.1.4 Plume Aerosol Optical Properties	17
2.2.1.5 Fire Plume Fluctuations	18
2.2.2 The Radiative Transfer Model	19
2.2.3 Fire Plume Turbulence Effects on Laser Beam Propagation	22
2.3 Model Implementation	25
2.3.1 FITTE: Fire Induced Transmittance and Turbulence Effects	25
2.3.1.1 Scenario 1	25
2.3.1.2 Scenario 2	26
2.3.1.3 Geometric Relations Used to Find Plume Parameters on the Line of Sight	28
2.3.1.4 General Information about Calculations along the Line of Sight	29
2.3.2 FGLOW: Fire/Fire Plume Radiant Emission and Transmittance	29
Caveats	30
3.1 Grade of Software	30
3.2 Model Failure	30
3.2.1 Cautions	30
3.3 Verification Tests	31
3.3.1 Fire and Plume Properties	31
3.3.2 Aerosol Optical Properties	32
3.3.3 Plume Distribution Functions	33
3.3.4 Effects of Thermal Plume Turbulence on Laser Beam Propagation	35
Operations Guide	36
4.1 Input	36
4.2 Output	43
4.2.1 Parameters Returned to the Calling Routine	43
4.2.2 Output Printed or Stored in Files	44
Sample Runs	45
5.1 Example 1: A scenario 1 calculation for a single wavelength	46
5.2 Example 2: A scenario 2 calculation for a single wavelength	47
5.3 Example 3: A scenario 1 calculation for a (visible) waveband	48
5.4 Example 4: A scenario 1 time-series calculation for a single wavelength	49
5.5 Example 5: A scenario 1 calculation with variation of fire parameters and with printout of spectrally resolved results for a selected instrument response function	51

5.6	Example 6: A single wavelength scenario 3 calculation	54
5.7	Example 7: A scenario 3 waveband calculation	56
5.8	Example 8: A time-series of scenario 3 calculations at a single wavelength	58
5.9	Example 9: Internal cycling with variation of wind direction to produce 5 output files.	60
	Acknowledgment	66
	References	67
	Appendix A: Auxiliary Programs to Aid Visualization of FGLOW Output	70
A.1	XS2PRT	70
A.2	XS2GRD	72
	Appendix B: Model Organization	73
B.1	Subroutines	74
B.2	Functions	76
	Appendix C: Fluctuation Time-History Data Files	78
C.1	Basic Ideas Underlying the Fluctuation Data Files	78
C.2	Construction of a Time-History File from Field Test Data	78
	Appendix D: Modification of Fire Parameters	80
D.1	Model Limitations on Fire Parameters	80
D.1.1	Developing Model Fire Parameters from Data	81
D.1.2	Checking Model Behavior When Varying Fire Parameters to Match Data	81

List of Figures

Figure 1. Side view contour plot of a fire plume in the model coordinate system. The plume edges shown are at the e^{-2} points of a conical Gaussian distribution. The centerline is sketched.	11
Figure 2. Plume distribution function behavior as a function of distance along the centerline from the fire.	14
Figure 3. Equivalent "top hat" and Gaussian distributions.	15
Figure 4. Contour plot of a space- and time-varying (4D) plume. Tic marks show 5 m spacing. The dashed line is the sketched centerline.	20
Figure 5. Geometry for the single line of sight scenarios. The helicopter would carry a laser designator for scenario 1 or a laser-guided munition for scenario 2.	26
Figure 6. Graphs of model output data for a time-series calculation at 10.6 μm . The dashed lines show the values predicted by the mean-value model.	27
Figure 7. Top view of scenario 3 (FGLOW) geometry. Situation shown is for 240 degree wind direction of Example 9.	29
Figure 8. Comparison of measured and modeled plume elevation angles.	32
Figure 9. Comparison of measured (Bruce et. al., 1991) and modeled extinction coefficients.	32
Figure 10a. Transmittance plots created with data from the example 8 simulation. Wavelength was 10.6 μm . Tic spacing is 5 m.	59
Figure 10b. Radiance plots created with data from the example 8 simulation. Wavelength was 10.6 μm . Tic spacing is 5 m.	59
Figure 11. Apparent temperature plots for various wind directions indicated. Prepared from the data files of the example 9 simulation. Wavelength was 3.6 μm	65
Figure A1. A pseudo-greyscale print of plume optical density produced with XS2PRT.	71
Figure B1. Diagram of FITTE model structure. Dashed lines indicate conditional calls. Functions, except EXPOF, listed in parentheses inside boxes.	73

List of Tables

Table 1. Values Defining Model Fires	9
Table 2. Particulate Optical Parameters	18
Table 3. Comparison of Albedo Values	33
Table 4. The REFD Card	36
Table 5. The SCEN Card	37
Table 6. The SRCL Card	37
Table 7. The METD Card	38
Table 8. The DETD Card	38
Table 9. The TARG Card	38
Table 10. The MOLS Card	39
Table 11. The BAND Card	39
Table 12. The OPT1 Card	40
Table 13. The SCN3 Card	41
Table 14. The TCAL Card	41
Table 15. The SVAR Card	42
Table 16. The GO Card	42
Table 17. The DONE Card	43
Table 18. Run times for selected run conditions	43

Chapter 1

Introduction

The Fire-Induced Transmission and Turbulence Effects (FITTE) module predicts transmittance through fire plumes, path radiance from fires/fire plumes and, optionally, effects of fire/fire plume turbulence on laser propagation for a given line of sight (LOS). The FGLOW model option extends the calculations to multiple lines of sight to predict the radiant image of a fire/fire plume segment that will be seen by an imaging system. The fires represent localized sources of burning diesel fuel, motor oil, and rubber, that is, simulated burning vehicles. FITTE also predicts the line of sight path-integrated particulate concentration, and, if a target temperature is specified, the attenuated thermal radiance from the target at the observer position. If the calculation is performed for a single wavelength, the model predicts beam spread and wander on a laser beam of that wavelength. The FGLOW option performs calculations for a set of lines of sight and creates a file of path radiance values, which represent the radiant image that would be seen by an imaging system, and of transmittance values, which represent the attenuation of the background image. An option allows output of an apparent temperature image.

1.1 Names of Things

1.2 Availability

1.2.1 Mailing Address

1.2.2 Phone and Electronic Mail

Chapter 2

Background

The FITTE and FGLOW models were developed to provide relatively rapid calculations of the effects of battlefield fires on detection, laser-designator and weapon systems. Earlier versions of these models treated the fire and fire plume as static mean-value entities.

Although much work has been done on modeling laser propagation in the atmosphere, the situations modeled were those for which homogeneous, isotropic turbulence could be assumed. These assumptions permitted simplifications in calculation of short- and long-time average spot size and average centroid jitter that are not valid for propagation through a fire plume.

Fire plumes are regions of space where there are rapidly changing atmospheric conditions. Special algorithms are needed to treat the effects of fire plume turbulence on propagation because of the rapid changes in refractive index within the plume, the large and non-uniform increase in the refractive index structure 'constant', and the fact that the turbulence effects depend on path-weighted turbulence parameters.

A preliminary model of the effects of a vertical fire plume on laser propagation was developed (Thompson and DeVore, 1981) for the US Army Atmospheric Sciences Laboratory. This model was modified (Bruce, Sutherland and Larsen, 1982) to handle bent-over plumes with obscuration from smoke for EOSAEL 82. The model predicted transmittance through the plume for a given line-of-sight and wavelength, and it optionally predicted magnitudes of beam wander and beam spread. The transmittance depended only on the plume aerosols since the major gaseous effluents, water vapor and carbon dioxide, are responsible for less than five percent of the total extinction in the visual and infrared atmospheric window regions of the spectrum where many Army systems operate.

Fire and plume parameters (fire temperature and plume vertical velocity) were obtained from field measurements (C. W. Bruce, private communication, 1982). Smoke optical parameters were obtained by a semi-empirical approach. A theoretical approach to determining specific extinction coefficients for carbonaceous aerosols has been described (Chylek et. al., 1981). This entails assuming equivalent spheres with appropriate particle-to-void ratios and applying Mie scattering theory. For the FITTE model, particle-to-void theory was modified to give agreement with transmissometer data (Sutherland and Walker, 1982; Sutherland et. al., 1984).

Minor changes were made in the FITTE model for EOSAEL 84. These were primarily changes to the calculation of radiative transfer. Model output was expanded to include attenuated target radiance from a 'hot' target and path radiance. This made it possible to predict target contrast.

The Forschungsinstitute für Optik commissioned the development of the FEUER code (Manning, 1985), a modification of the 1984 version of FITTE that added effects of absorption and emission by the major effluent gases to the predictions and that also added the capability to perform calculations over a waveband. The work was based on modification of code from the ATLES model (Young, 1977). Temperature dependent values of absorption coefficients are included for water vapor in the spectral region from 2.222 to 200.000 μm (4500 to 50 cm^{-1}), and for carbon dioxide in the regions from 2.702 to 3.225 μm (3700 to 3100 cm^{-1}) and 4.160 to 5.000 μm (2400 to 2000 cm^{-1}). Data are included for temperatures from 100 to 3000 K. This code was supplied to the Atmospheric Sciences Laboratory and was incorporated into the EOSAEL 87 version of the model.

The FGLOW model (Bruce, 1988) also was added for EOSAEL 87. FGLOW is an extension of FITTE that performs transmittance and path radiance calculations for a set of lines-of-sight in a rectangular array. The output can be used to predict the mean image of the fire/fire plume that would be seen by an imaging sensor.

Significant changes were made for the first revision of EOSAEL87 FITTE. Some changes result from work done (to increase the speed of calculation) for the Forschungsinstitut für Optik by OptiMetrics, Inc. (Manning and Kebscull, 1988) and other changes result from work at the Atmospheric Sciences Laboratory. Most of the changes are transparent to the user. They cause an increase in the speed of calculations, by up to a factor of 10, particularly for waveband and for FGLOW image calculations.

Time-dependent spatial variations have been added to the FITTE/FGLOW model for EOSAEL 92. This was accomplished by adding time-dependent fluctuations to the centerline position and to most the mean-value Gaussian-distributed parameters. Other changes include options to perform time-series calculations and to vary one or more of the fire parameters.

2.1 Conceptual Overview of FITTE

Simplified physical models of fires and fire plumes are combined with a model for radiative transfer to predict the effects on propagation. A specially tailored model of the turbulence structure function within a fire plume is used to predict beam spread and wander for laser propagation. Empirical data is used for fire and aerosol parameters.

2.2 The Physical Models

2.2.1 The Fire and Fire Plume Models

The fire and fire plume are described in terms of mean time-averaged parameters with time-varying fluctuations added to create dynamical variation. The mean value description will be given first, and will be followed by a description of the fluctuation modeling.

2.2.1.1 The Time-averaged Fire

FITTE/FGLOW uses an extremely simple model for the fire itself. A fire is modeled as a circular disk with fixed mean temperature, T_o , radius, R_o , and burn time, t_{burn} and specific quantities of fuel.

The fire is centered at the origin of the model coordinate system that is a right-handed coordinate system with the positive x-axis coinciding with the downwind direction. This coordinate system will be used for the description of the models since it affords the simplest possible equations.

The user specifies a fire type from several types that represent burning vehicles or vehicular fuels. The model is restricted to these fires because they are the only type of fuel mixture on which a relatively complete set of data is available.

The fire characteristics were chosen based on data from the Battlefield Induced Contamination Tests, BICT I and BICT III. They were designed to give realistic values for mean heat and aerosol fluxes. Types 1, 2 and 3 correspond roughly to small (jeep), medium (truck), and large (tank) burning vehicles, while type 4 is a larger fire that represents a small fuel depot. They should be reasonable representations of battlefield fires. Table 1 lists defining values for the fires.

Table 1. Values Defining Model Fires

	Type	Diesel Fuel (gal)	Motor Oil (qt)	Rubber (kg)	Radius (m)
Jeep	1	5	6	40	0.6
Truck	2	20	8	100	1.0
Tank	3	125	16	250	2.0
Fuel Depot	4	800	160	0	4.0

Quantities derived from the source parameter values are the aerosol (smoke) mass emission rate, the heat emission rate, and the number densities of the major molecular combustion products (carbon dioxide and water vapor). These values are converted to fluxes through the plume cross-sectional area.

Calculation of the aerosol mass emission rate, Q_M , requires a value for the particulate emission factor, E_f , which is the ratio of the mass of particulates produced to the mass of fuel consumed in the combustion process. This quantity is difficult to determine and is estimated, from experimental data (Sutherland and Walker, 1982), to be 0.160 g/g. The mass emission rate is modeled as

$$Q_M = E_f \frac{M_{DF} + M_{MO} + M_{RU}}{t_{burn}} \quad (1)$$

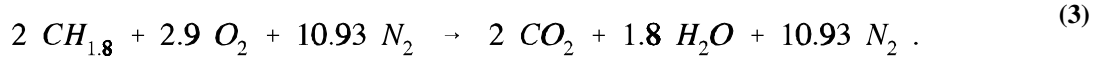
where the M 's are the total mass (in grams) of diesel fuel (DF), motor oil (MO), and rubber (RU) and t_{burn} is the total burn time, which is set equal to 25 minutes to obtain heat and mass flux levels similar to those at the BICT tests.

The heat emission rate, Q_H , is given by

$$Q_H = (1 - E_f) \frac{E_{DF} M_{DF} + E_{MO} M_{MO} + E_{RU} M_{RU}}{t_{burn}} \quad (2)$$

where the E 's are the heats of combustion of the various fuels. The factor $(1 - E_f)$ arises to account for the fact that particulates are unburned residue of the combustion process. Values for the heats of combustion have been summarized (Gomez et. al., 1980) from data (Turner et. al., 1980; Levitt and Levitt, 1982).

The molecular concentrations (# molecules/cc) of the major combustion products are arrived at as follows. Combustion of diesel fuel is represented (Leslie et. al., 1980) by



This reaction is a composite representation of a set of reactions, one for each of the various fuel molecules. Although the reaction above is generally used to approximate combustion in an engine, it is equally valid for combustion in air. The molecular concentration of carbon dioxide due to combustion, C_{S1} , in a 1 cm high volume above a fire of area a_F cm² is

$$C_{SI} = \frac{\text{hydrocarbon fuel weight}}{\text{molecular weight of } CH_{1.8}} \cdot N_A \cdot \frac{1}{t_{burn}} \cdot \frac{1}{a_F \cdot s_o}, \quad (4)$$

where N_A is Avogadro's number, and s_o is the effluent velocity (cm/s) just above the fire. From Eq. 3, the molecular concentration of water vapor, C_{S2} , produced by combustion is 0.9 times that of carbon dioxide.

The mean temperature (923.16 K) for the "top hat" fire distribution was chosen based on unpublished data taken by the author during the Battlefield Induced Contamination Tests I (Kennedy, 1981). This translates to a peak temperature of roughly 2000 K for the equivalent Gaussian distribution used in the model.

2.2.1.2 The Time-averaged Fire Plume

FITTE uses a "top hat" plume model to describe the transport of general curved plumes as well as the special cases of horizontal and vertical plumes. The "top hat" distribution is simply one that has a single value within the plume radius and is zero outside the plume.

The "2/3 law" model (Briggs, 1969) is used to predict the time-averaged plume centerline. The plume centerline equation for a finite source at the origin of the coordinate system is

$$z + z_V = \frac{C}{U} (x + x_V)^{2/3}, \quad (5)$$

where x and z are plume centerline coordinates in the x - z plane, x_V and z_V are constant coordinates of a virtual point source and are chosen to match boundary conditions at the fire source, and U is the ambient mean windspeed (assumed uniform with height). U is not permitted to be less than 0.10 m/s to ensure that Eq. 5 is well defined. Figure 1 shows a time-averaged plume in the model coordinate system.

The constant C is given by

$$C = \left(\frac{3F}{2\xi^2} \right)^{1/3}, \quad (6)$$

(Weil, 1981) where ξ is an entrainment constant, that is, a constant that describes the fractional increase in plume volume per unit distance along the centerline caused by diffusion. F is the buoyancy flux, defined as

$$F = \frac{gQ_H}{\pi C_P \rho_A T_A} = g W_o R_o^2 \frac{(T_o - T_A)}{T_o}, \quad (7)$$

g is the gravitational acceleration, Q_H is the source heat flux, C_P is the specific heat of air at constant pressure, ρ_A is the ambient air density, T_A is the ambient temperature, T_o is the source temperature, W_o is the initial plume vertical velocity, and R_o is the source radius.

If it is assumed that the buoyancy flux is conserved, Eq. 7 will apply at any height z if the values T_o , W_o and R_o are replaced by $T(z)$, $W(z)$ and $R(z)$.

Using a geometrically based argument similar to those in the literature (Hoult, Fay and Forney, 1969), the entrainment parameter ξ for a general plume can be expressed as

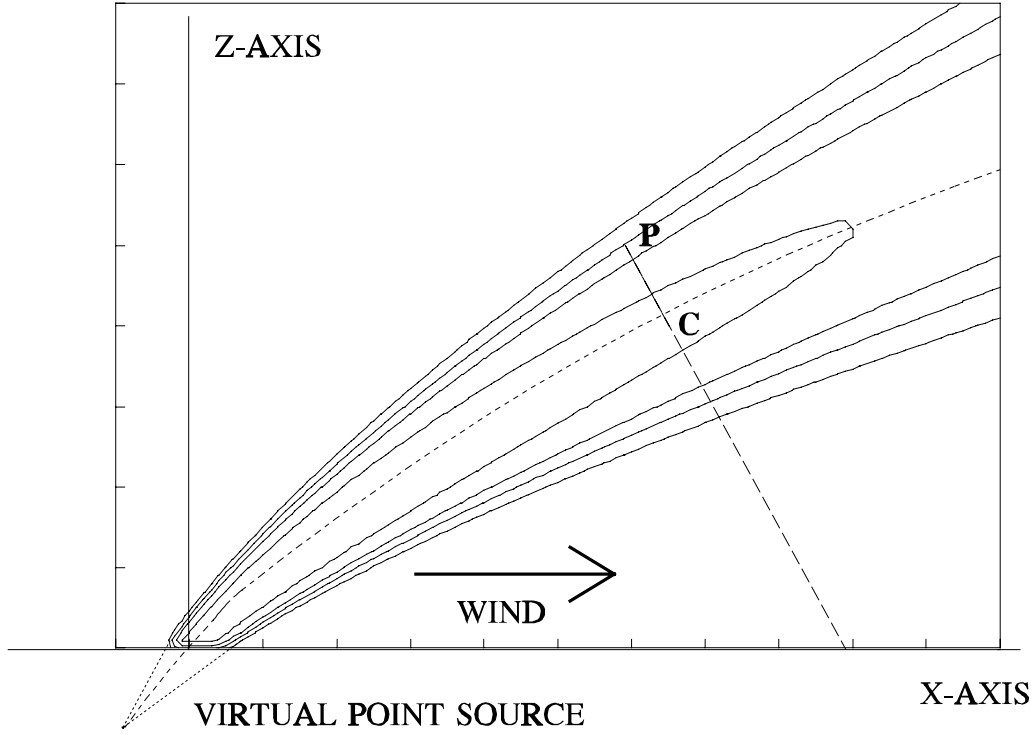


Figure 1. Side view contour plot of a fire plume in the model coordinate system. The plume edges shown are at the e^{-2} points of a conical Gaussian distribution. The centerline is sketched.

$$\xi = \eta \left[1 - \left(\frac{U}{S} \right)^2 \right] + \upsilon \left(\frac{U}{S} \right)^2, \quad (8)$$

where η is the empirically determined entrainment constant for a vertical plume, υ is that for a horizontal plume, and S is the plume velocity along the centerline. Experimentally determined values chosen for entrainment into vertical and horizontal plumes are $\eta = 0.12$, and $\upsilon = 0.60$, respectively (Hoult and Weil, 1972) although values have been reported (Briggs, 1969) as low as 0.07 for vertical plumes and as high as 1.0 for horizontal plumes. ξ must be constant to maintain model simplicity, so the value of plume velocity at the origin, $S(0)$, is used in the defining equation.

The mean velocity along the centerline, S , is assumed to be the vector sum of the ambient mean wind vector U , and the mean vertical plume velocity W . S and W may be written as functions of z , or alternatively in terms of D , the distance from the origin along the centerline. The time-averaged plume parameters, which are assumed to have Gaussian distributions about the plume centerline (George et. al., 1977), are most easily expressed as functions of D and of the plume width parameter $\sigma(D)$.

The relation between the value of the centerline coordinate z and the distance D of that point from the origin is obtained as follows. The ambient wind is assumed to be horizontal, so $W(z)$ can be expressed as

$$\frac{W(z)}{U} = \frac{(dz/dt)}{(dx/dt)} = \frac{dz}{dx} \quad (9)$$

at any point on the centerline. Substitution for dz/dx from the plume centerline equation gives

$$W(z) = \frac{2}{3} C^{3/2} \frac{1}{\sqrt{U(z + z_V)}} \quad (10)$$

Since the vertical wind velocity at the origin, W_o , is known and ξ is defined in terms of known quantities, the constants z_V , x_V , and C can be found.

The plume model assumes that the time-averaged plume parameter distributions vary as functions of D . It is therefore usually more convenient to express the parameters as functions of D rather than of centerline height z . The relationship between D and z is found by integrating

$$dD = \sqrt{(dx/dz)^2 + 1} dz \quad (11)$$

from the origin to the point of interest along the centerline, z_{Cl} . This gives

$$D = \left(\frac{2C}{3U} \right)^3 \left[\sqrt[3/2]{(z_{Cl} + z_V) \left(\frac{9}{4} \right) \left(\frac{U}{C} \right)^3 + 1} - \sqrt[3/2]{z_V \left(\frac{9}{4} \right) \left(\frac{U}{C} \right)^3 + 1} \right] \quad (12)$$

2.2.1.3 Time-Averaged Plume Effluent and Temperature Distribution Functions

Spatially resolved measurements of time-averaged plume parameters such as temperature and vertical velocity can be described by circularly symmetrical Gaussian distributions (Hoult et. al., 1969). Such distributions are used to describe the mean values of the temperature, effluent concentrations (of aerosols and molecular combustion products), and the vertical velocity of the plume when calculations are performed to predict the transmittance and turbulence effects. For a vertical plume, such a distribution has the form

$$A_d(r, z) = A_d(0, z) \cdot e^{-\frac{r^2}{2(\sigma(z))^2}} \quad (13)$$

where $A_d(0)$ represents the parameter amplitude, r the radial distance from the centerline, and $\sigma(z)$ the diffusion function.

The distribution functions remain the same for the general curved plume used in FITTE but their mathematical description becomes more complex. Conservation assumptions determine the decrease in peak amplitude of the parameters as a function of distance along the centerline. The general behavior of the plume distribution functions is shown in Fig. 2.

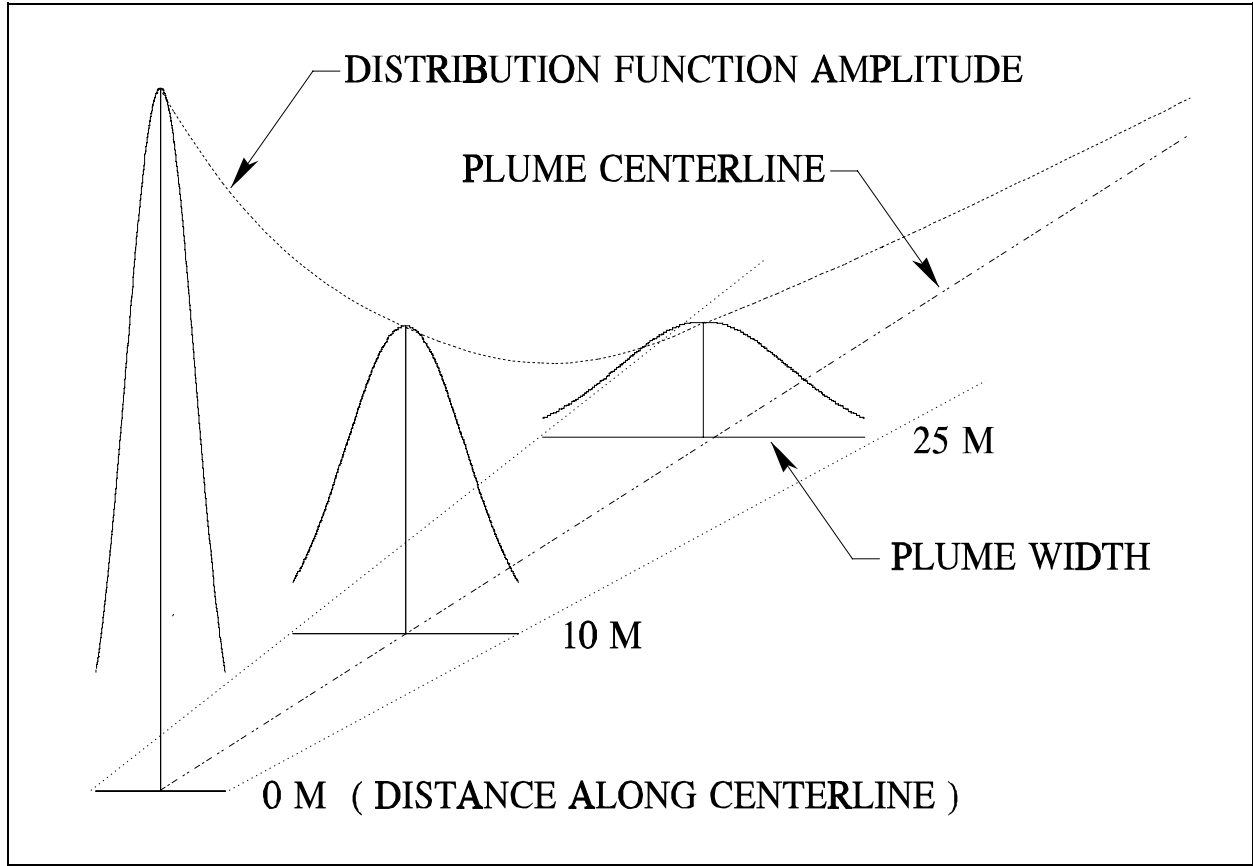


Figure 2. Plume distribution function behavior as a function of distance along the centerline from the fire.

The diffusion function, σ , is related to the entrainment parameter by

$$\sigma(D) = \sigma(0) + \frac{\xi D}{6.06}, \quad (14)$$

and to the plume radius, R , by

$$R = 2.0 \sigma(D). \quad (15)$$

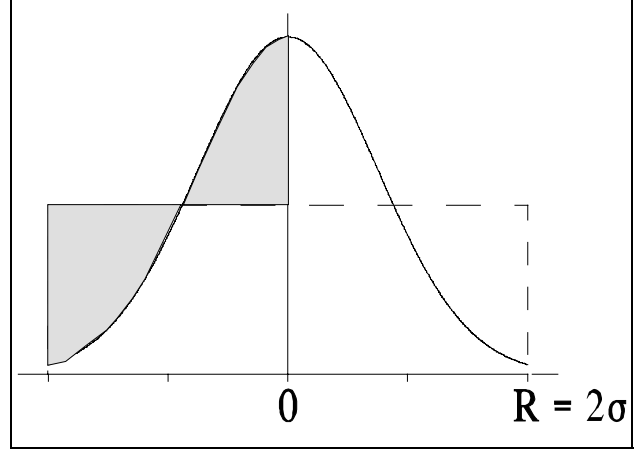
This definition of the plume radius agrees roughly with the apparent plume edge seen by an observer. In performing the propagation integrals, FITTE actually uses the plume parameter distribution functions whenever a LOS point is within 3σ of the centerline, that is, until the parameter has fallen to approximately 1% of its peak value. The same radius is used for all of the plume parameters.

The relation between equivalent "top hat" and Gaussian plume distributions has been described elsewhere (Thompson and DeVore, 1981). For equivalent distributions, the integrated "top hat" values of mass, momentum and buoyancy are required to equal truncated integrals of the corresponding Gaussian plume parameters. Figure 3 shows "equivalent" distributions, with the shaded portions in the left half indicating the areas mapped by the transformation between the distributions. The maximum of the Gaussian distribution is approximately 2.31 times the "top hat"

amplitude for the effluent densities. The relation for the excess temperature above ambient is more complex and the ratio ranges from about 2.3 to 2.9.

The equation used to describe effluent aerosol concentration is based on that for a classic horizontal Gaussian plume; that is,

$$\chi(x, y, z) = \frac{Q_M}{2\pi U \sigma^2} e^{-\frac{y^2}{2\sigma^2}} \left[e^{-\frac{z^2}{2\sigma^2}} + e^{-\frac{(z+z_c)^2}{2\sigma^2}} \right] \quad (16)$$



where χ is the aerosol concentration at any point specified in the model coordinate system. Q_M is the aerosol mass emission rate, U is the mean ambient wind velocity, $\sigma(x)$ is the diffusion function, and z_c is the height of the plume centerline at x . The effluent molecular combustion product concentrations are described in similar fashion.

Figure 3. Equivalent "top hat" and Gaussian distributions.

Equation 16 applies only in the extreme case of a horizontal plume. To include plume curvature or a vertical plume, the equation must be modified so that the parameters are related to the direction of the mean flow at any point along the centerline. This transformation, although simple in principle, introduces geometrical and mathematical complexities since the direction of the mean flow vector is a function of location for a curved plume.

For the general curved plume, the analogue of Eq. 16 is

$$\chi(D, h, y) = \frac{2.31 Q_M}{4\pi S \sigma^2} e^{-\frac{y^2}{2\sigma^2}} \left[K_1 e^{-\frac{h^2}{2\sigma^2}} + K_2 e^{-\frac{(2h_c + K_3 h)^2}{2\sigma^2}} \right], \quad (17)$$

where D is the distance along the plume centerline to a point $(x_{cl}, 0, z_{cl})$, h is the distance (measured perpendicular to the mean flow vector S at D) from the plume centerline to the projection of a point on the line-of-sight $(x_L, 0, y_L)$ onto the x - z plane, h_c is the distance of the plume centerline from the ground (also measured perpendicular to S at D), and $\sigma(D)$ is related to the plume radius at D as illustrated in **Fig. 2**. The coordinate y is the distance from the plume centerline perpendicular to the x - z plane.

The constants K_1 , K_2 and K_3 in Eq. 17 take on values appropriate for specific situations. For a horizontal plume $K_1 = K_2 = 1.0$. For a vertical plume $K_1 = 1$ and $K_2 = 0$. These constants account for the fact that there is reflection from the ground for quasi-horizontal plumes. The conditions under which the model changes from one set of these values to the other for bent-over plumes is described later. When there is reflection, K_3 is set equal to +1, if the point at which the function is to be evaluated lies above the centerline, or to -1, if the point lies below the centerline, to obtain the appropriate value for the reflected concentration.

An accurate description of the plume temperature distribution is needed for calculations of the turbulence effects. If values from the equation for pressure equilibrium,

$$\bar{\rho}(r) \cdot \bar{T}(r) = \rho_A \cdot T_A = \rho_o \cdot T_o , \quad (18)$$

are substituted into the equation for the equivalence of mass,

$$\pi \bar{\rho} R_{TH}^2 = \int_0^{R_{TH}} 2\pi \rho(r) r dr , \quad (19)$$

the centerline temperature increment above ambient can be determined for an "equivalent" truncated Gaussian plume (one for which the integral of the "top hat" distribution is equal to the integral of the truncated Gaussian distribution). Overbars indicate the mean values associated with the "top hat" model. Experiments indicate that "equivalence" of the distributions should be defined for a "top hat" radius $R_{TH} = 2.0 \sigma(D)$, which corresponds roughly to the visible edge of the plume. This definition leads to the expression for the centerline temperature

$$T_C(z) = T_A \frac{[e^2 - 1]}{[e^{2T_A/\bar{T}} - 1]} . \quad (20)$$

The relations between the peak and mean values of the effluent concentration and the vertical velocity are found in a similar manner. It is assumed that all of these distributions are characterized by the same plume radius. Experiments indicate that this assumption is approximately correct.

Finally, the gradient of the amplitude of the plume temperature distribution must be found as a function of distance D along the centerline (or, alternatively, as functions of the centerline height z) for use in the turbulence effects calculations. This is done by expressing the centerline temperature as a function of z and taking the derivative with respect to z to obtain

$$\frac{dT_C}{dz} = \frac{dT_C}{d\bar{T}} \cdot \frac{d\bar{T}}{dz} \quad (21a)$$

where

$$\frac{dT_C}{d\bar{T}} = 2 \left[\frac{T_A}{\bar{T}} \right]^2 (e^2 - 1) \frac{e^{2T_A/\bar{T}}}{[e^{2T_A/\bar{T}} - 1]^2} \quad (21b)$$

and

$$\frac{d\bar{T}}{dz} = T_A g F \left(\frac{2 C^{3/2} R^2 z^{-1/2} + 6 \xi U^{3/2} W R}{3 U^{3/2} (F - g W R^2)^2} \right) . \quad (21c)$$

R and W have been treated as explicit functions of z in arriving at Eq. 21c and are treated as such in its evaluation.

The change in amplitude of the effluent flux distributions as functions of D are found by observing that the mass flow through all plume cross sections must remain constant to prevent buildup of mass at any location, so that at

any distance D from the origin the effluent flux must be equal to the initial flux times the product of the plume velocity S and the cross sectional area at the origin divided by the same product evaluated at distance D .

2.2.1.4 Plume Aerosol Optical Properties

Visual and infrared aerosol optical parameters were based on theoretical calculations modified to give agreement with transmissometer data from the Battlefield Induced Contaminants Test, BICT I. The aerosol specific extinction coefficients, α , for various wavelengths were based on Mie scattering theory calculations. These calculations used a theory (Chylek et. al., 1981) that assumes that carbon-based aerosols can be replaced by equivalent spheres with appropriate particle-to-void ratios. The theory was modified to give agreement with ratios of measured transmittance for different wavelengths. Details are given elsewhere (Sutherland and Walker, 1982; Sutherland et. al., 1984) and will not be repeated here.

The values of single scattering albedo, ω , were taken from measurements (C. W. Bruce, private communication, 1981) or from Mie calculations (Khanna and Ammon, 1983) for aerosol size distributions and porosity characteristics based on measurements (Pinnick et. al., 1982).

Table 2 lists the values used in FITTE. Interpolation is used to calculate the specific extinction coefficient and albedo at intermediate wavelengths. The millimeter wavelength values are from measurements (C. W. Bruce, private communication, 1982).

Table 2. Particulate Optical Parameters

Wavelength (μm)	Specific Extinction Coefficient (m^2/g)	Single Scattering Albedo
0.40	7.41	0.25150
0.55	5.57	0.25000
1.06	2.94	0.24493
1.50	2.23	0.24055
2.50	1.61	0.23060
3.80	1.34	0.21766
6.00	1.14	0.19577
8.50	1.01	0.17090
10.60	1.00	0.15000
8570.00	0.002	0.00000

2.2.1.5 Fire Plume Fluctuations

The space-time variation of the fire plume is handled as a two-part model. The fluctuations of the plume about the mean centerline are treated as functions of wind-speed and wind-direction fluctuations, while the fluctuations of the plume parameters are based on the assumption that they are dependent on turbulent mixing.

A time history data file, FIT4D.DAT, is used to store the information needed for the fluctuation model in FITTE/FGLOW. This file contains two thousand rows and three columns of data. The rows of data have a one second time increment and represent a time history of wind fluctuations since the start of the fire. Column 1 contains a random number (range: -0.5 to 0.5) that is used as input for calculating plume parameter fluctuations at a given time, column 2 contains the normalized cumulative fluctuation of the downwind (x-) component of the wind, and column 3 contains the normalized cumulative fluctuation of the crosswind (y-) component of the wind. The model was developed and tested with simulated data. Files developed from actual wind data will be furnished and should be used after model operation has been checked. Details will be given in a file README1.FIT. The file structure is discussed further in Appendix C where information is given on creating a time history file from wind data.

When FITTE is run a current time is assigned. This may be the default time (100 seconds after the start of the fire) or another time that is read from an input card.

The displacement of any point P on the centerline from its mean position at the current time is calculated in the following way. The distance along the mean centerline from the origin to point P is calculated using Eq. 12. The average plume velocity \bar{S} to reach point P is half the sum of $S(P)$ and $S(0)$. The ratio of distance to mean velocity gives the time taken to reach point P from the fire. This is used to assign a source time, that is, the time when the plume segment currently at point P left the source. The current time and source time are used as pointers to rows of the data array. Using the second (or third) column of the array, the difference in value between the values in these rows multiplied by the mean windspeed U gives the x- (or y-) displacement of the point P from the mean centerline position. This permits the current position of point P to be calculated and to be used to determine the plume parameter distributions at points on a LOS near point P. Interpolation takes place when the time to reach point P is not an integer.

The random numbers in the first column of the FIT4D.DAT file are used in two separate ways. The first way assigns scaled fractional fluctuations to the plume radius and to the heat and effluent production. The scaling limits the fluctuations to no more than five percent of the mean value of the corresponding parameter.

The second way that these numbers are used is as input for calculation of the fluctuations of the aerosol and effluent gas concentrations and of the plume temperature. Modeling of these plume parameter fluctuations is based on the assumption that they are driven by atmospheric turbulence. They should therefore exhibit the same power spectral density distribution as is found for atmospheric parameters within an appropriate frequency range. This is achieved by the choice of the coefficients used for the series that describes the fluctuations. The fluctuations are represented by a series with the form

$$\delta = \sum_{k=1}^n c_k \cos(b^k x + \phi_k) . \quad (22)$$

The phase angles, ϕ_k , for the terms are obtained from the random numbers stored in the first column of the FIT4D.DAT file. Figure 4 is an example of a space- and time-varying (4D) plume.

2.2.2 The Radiative Transfer Model

The radiative transfer equation for a medium in which aerosol scattering and absorption and molecular absorption all occur is

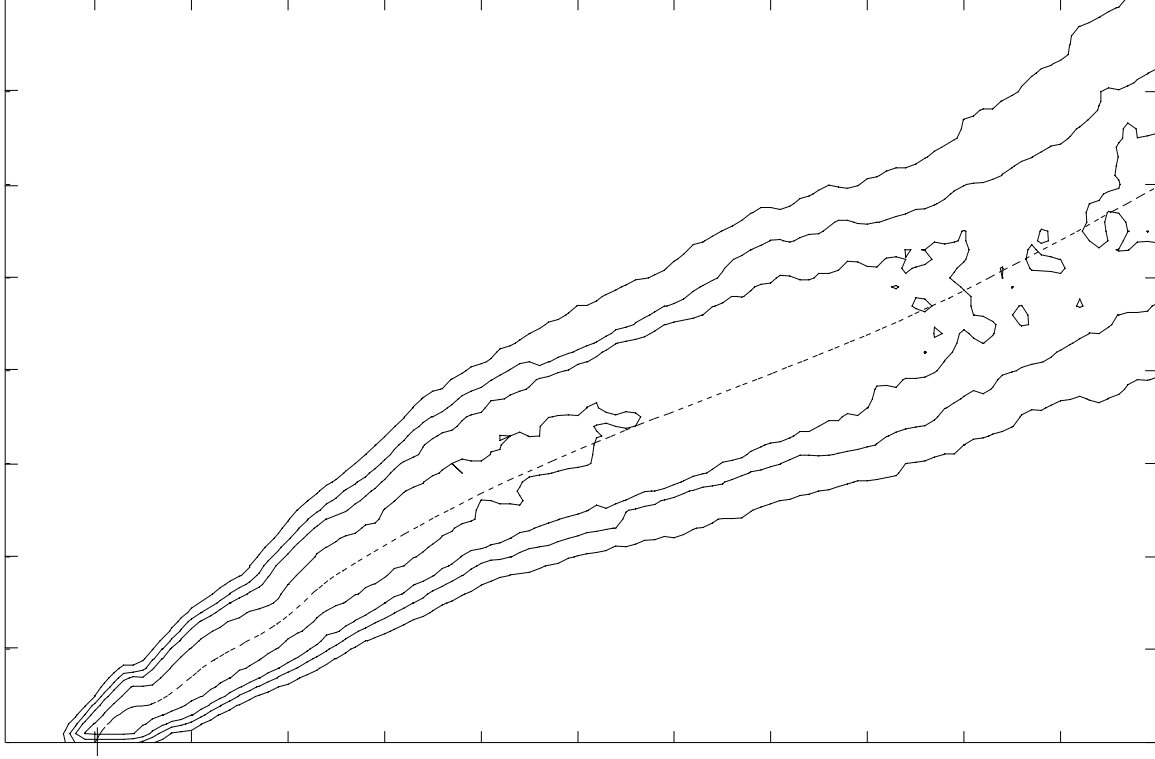


Figure 4. Contour plot of a space- and time-varying (4D) plume. Tic marks show 5 m spacing. The dashed line is the sketched centerline.

$$\frac{dI}{ds} = -\epsilon I + (\kappa_A + \kappa_M)B \quad (23)$$

where I is the local spectral radiance ($\text{W}/\text{m}^2/\text{sr}/\text{cm}$), s is distance along the line of sight, ϵ is the total extinction coefficient (m^{-1}), κ_A and κ_M are the aerosol and molecular absorption coefficients (m^{-1}), and B is the blackbody function,

$$B(\lambda, T) = \frac{2\pi h c^2}{\lambda^5} \left[\frac{1}{e^{hc/\lambda k T} - 1} \right]. \quad (24)$$

Here h is Planck's constant, k is Boltzmann's constant and c is the speed of light in vacuum. Note that the radiance, I , has units of $\text{watts}/\text{m}^2/\text{steradian}/\mu\text{m}$, and the blackbody irradiance, B , has units of $\text{watts}/\text{m}^2/\mu\text{m}$.

For the aerosol, the absorption coefficient κ_A is related to the extinction coefficient ϵ by

$$\kappa_A = (1 - \omega) \varepsilon = (1 - \omega) \alpha \chi , \quad (25)$$

where α is the specific mass extinction coefficient of the aerosol (m^2/g), ω is the single-scattering albedo, and χ is the local aerosol concentration (g/m^3).

In FITTE, only the effluent aerosol and the major molecular combustion products (water vapor and carbon dioxide) are considered in the calculation. The aerosols are the dominant specie for calculations in the visible and infrared atmospheric window regions (Sutherland and Walker, 1982 and Khanna et. al., 1982). If the path from target to observer is treated as a series of segments for which the effluent concentrations and temperature are nearly homogeneous, the radiative transfer equation can be integrated for each path segment to give

$$I = I_s e^{-\tau} + \frac{1}{\pi \varepsilon} \left[(1 - \omega) \alpha \chi + \kappa_A B(1 - e^{-\tau}) \right] , \quad (26)$$

where τ is the optical depth of the segment, I is the spectral radiance in the segment, and I_s is the spectral radiance entering the segment from all previous segments. The radiative transfer calculation is performed by evaluating this expression for each segment from the target to the observer, using I for each segment as I_s for the next segment.

The extinction coefficients are functions not only of wavelength, but also of temperature. The values used for the aerosol are temperature-average values from measurements; those for the molecular combustion products are temperature dependent and are taken from the ATLES model (Young, 1977) and from unpublished data.

Both the transmittance through the gaseous effluents of the fire plume and the molecular contribution to the path radiance are calculated by a band model adapted from the ATLES code (Manning, 1985). For single wavelength calculations the waveband used is extremely narrow. The spectral resolution is not high but is dependent on the band model data base used, and is generally 25 cm^{-1} . An important feature of the ATLES band model is its ability to treat temperature dependence if the data base used contains parameters for high temperatures. This is the primary reason for choosing this model rather than the LOWTRAN code (Kneizys et. al., 1983).

The band model was extracted from the ATLES code and adapted for use in FITTE. Code to perform calculations through aircraft and missile plumes was removed, large arrays were reduced in size by limiting the number of species the code can handle simultaneously and by limiting the size of the data base files that can be loaded, and the parts of the code that handle Doppler and Voigt lineshapes were eliminated since only Lorentz lineshapes are needed for FITTE.

The importance of temperature dependence has been described (Manning, 1985). He points out that, at high temperatures, transmittance is not strongly affected in the 2500 cm^{-1} region but it is greatly reduced in the 2000 cm^{-1} and 3300 cm^{-1} regions as hot-band transitions from nearby carbon dioxide and water vapor bands become active. Since the radiance emitted in a spectral band increases as transmittance decreases, correct prediction of transmittance in the fire plume is important.

The band model parameters included for use in FITTE are taken from four files, two for carbon dioxide and two for water vapor. They have been combined into a single file called BPARAM.DAT. The carbon dioxide section of the file covers the spectral region 2000 to 2400 cm^{-1} , which includes the important carbon dioxide fundamental band at $4.3 \mu\text{m}$ (2300 cm^{-1}), and the region from 3100 to 3700 cm^{-1} . It includes temperature data at ten temperatures from 100 K to 3000 K . The water vapor section of the file covers the spectral regions from 50 to 2500 cm^{-1} and from 2500 to 4500 cm^{-1} . It contains data at seven temperatures between 300 K and 3000 K . This file

represents most of the important absorption bands of carbon dioxide and water vapor in the infrared. The carbon dioxide files used were supplied with the ATLES code. The water vapor files used are later, unpublished data.

When the input specifies that calculations are to be performed for a spectral band, the radiance is integrated over the band, and the transmittance is averaged over the band. These calculations are made using the equations below.

If $I(\nu)$ represents spectral radiance ($\text{W/m}^2/\text{sr/cm}$), and $f(\nu)$ represents an instrument spectral response function with a range of zero to one, the integrated radiance is given by

$$I = \int I(\nu) f(\nu) d\nu , \quad (27)$$

and has units of $\text{W/m}^2/\text{sr}$. The average transmittance over the band is

$$\bar{\tau} = \frac{\int I(\nu) f(\nu) d\nu}{\int f(\nu) d\nu} . \quad (28)$$

Note that these are two different types of calculation. The radiance is an integrated quantity; if the radiance is constant with wavenumber and the instrument response function is a rectangular function, increasing the size of the rectangular window should increase the radiance. The transmittance is an average over the band; if the transmittance is constant with wavenumber and the size of the rectangular window is increased, the average transmittance should not change.

2.2.3 Fire Plume Turbulence Effects on Laser Beam Propagation

Prediction of the effects of fire plume turbulence on propagation requires the use of a stochastic model. The turbulent hot plume can be regarded as a variable density lens that changes with time. The driving forces for the fluctuations are entrainment and turbulent mixing of ambient temperature air into the plume. It is assumed that existing theory for laser beam propagation through the turbulent atmosphere can be used if appropriate changes are made to the definitions of parameters and the ranges in which they are valid. The key assumption is that the index of refraction structure constant, C_n^2 , must be replaced by a structure function within the plume that is dependent on the time-averaged temperature distribution. The gradient of the time-averaged temperature distribution determines the step size that must be used to obtain accurate results from the calculations.

The turbulence effects model predicts values of laser beam parameters at the target that depend on the turbulence induced fluctuations in the LOS index of refraction. The magnitudes of the propagation effects are a complex function of the wavelength and of the relative sizes of the laser beam and the plume. It is a modification of a model developed (Thompson and DeVore, 1981) for the Atmospheric Sciences Laboratory based on work in the literature (Fante, 1975).

The index of refraction structure constant (Tatarski, 1971) is given by

$$C_n^2 = \frac{\langle [\tilde{n}(r_2) - \tilde{n}(r_1)]^2 \rangle}{(r_{12})^{2/3}} , \quad (29)$$

where $\tilde{n}(r_i)$ is the instantaneous fluctuation in index of refraction at point r_i , r_{12} is the distance between points r_1 and r_2 , and the brackets denote an ensemble average over all points (in a localized region) that are separated by the distance r_{12} . In practice, an ergodic hypothesis is invoked to replace the ensemble average by a time average.

The index of refraction of air is given by

$$n = 1.0 + 77.6 \times 10^{-6} \frac{P}{T} \left[1.0 + \frac{7.52 \times 10^{-3}}{\lambda^2} \right], \quad (30)$$

where P is pressure (millibars), T is temperature (Kelvin), and λ is the wavelength of interest (micrometers). A humidity dependent term that is negligible at visual and infrared wavelengths has been omitted. Examination of Eq. 30 shows that temperature fluctuations will cause index of refraction fluctuations.

For atmospheric turbulence, where the temperature fluctuations are of the order of one degree Kelvin, the variance of the index of refraction is proportional to the variance of the temperature. For turbulence in fire plumes, where temperature fluctuations are of the order of tens or hundreds of degrees, the variance of the index of refraction must be related to that of the reciprocal of the temperature, that is,

$$\sigma_n^2 = A_n^2 (\sigma_{1/T})^2, \quad (31)$$

where

$$A_n = (n - 1)T. \quad (32)$$

The index of refraction structure constant is then obtained from the relation

$$C_n^2 = 1.91 \left(\frac{\sigma_n^2}{L_o^{2/3}} \right), \quad (33)$$

where L_o is the outer scale of turbulence (Tatarski, 1971). In a plume, L_o is equal to the radius of the plume.

Effects of turbulence on propagation in the atmosphere are calculated using the assumption of a Kolmogorov spectral distribution of index of refraction fluctuations. L_o is the outer scale of turbulence (the size of the largest eddies for which the energy cascade to smaller eddies is linear), and l_o is the inner scale. For the atmosphere, L_o is of the order of tens of meters and l_o is of the order of millimeters.

For turbulence in fire plumes, the Kolmogorov spectral distribution is used with the outer scale, L_o , set equal to the radius of the plume. Values of C_n^2 inside the plume are typically one to three orders of magnitude higher than ambient values. To evaluate C_n^2 along the path, it is necessary to assume a temperature probability distribution about the mean temperature at any given point. The time-averaged temperature distribution in the plume, in a plane perpendicular to the centerline, is a circularly symmetrical Gaussian with the form

$$T = (T_C - T_A) e^{-\frac{r^2}{2(\sigma(D))^2}} + T_A, \quad (34)$$

where T is the time-averaged temperature at a point p , T_C is the centerline temperature, T_A is the ambient temperature, r is the distance of point p from the centerline, and $\sigma(D)$ is the diffusion function that specifies the local plume width. The centerline temperature is obtained from the plume model and the average temperature at point

p is used to predict the value of $C_n^2(p)$ that is used in the turbulence effects calculation. In actual calculations, the simplified exponential expression of Eq. 33 is replaced by the exponential terms of Eq. 17.

FITTE uses established turbulence theory (Fante, 1975) to find the diffraction limited spot radius (ρ_D), the lateral coherence length (ρ_o), the short- (ρ_s) and long-time (ρ_L) average spot radii, and the average instantaneous distance of the centroid (ρ_c) from its long-time average position. These parameters are used to predict a centroid jitter radius and a spot area magnification ψ .

The increase in the instantaneous beam area at the target is calculated from

$$\psi = \left(\frac{\rho_s}{\rho_D} \right)^2 \quad (35)$$

where ρ_D is the diffraction limited spot radius at the target. This result can be used to estimate the average decrease in intensity at the target. No detailed information about spot intensity distributions is predicted because these distributions are a function of relative beam size and plume size, the variations in path integrated particulate concentration for incremental areas of the spot and of the fluctuating lens represented by the plume.

For the points outside the plume, the value of C_n^2 is assumed to be constant and equal to $1.0 \times 10^{-14} \text{ m}^{-2/3}$, a moderately high atmospheric value. For plume temperatures less than 10 degrees C above ambient, an approximation is used to evaluate the variance of the index of refraction. For this case

$$\sigma_T^2 \approx 0.4 \left(\bar{T} - T_A \right), \quad (36)$$

(George et. al., 1977) where \bar{T} is the mean temperature at a point, and the approximate relation

$$\sigma_n^2 \approx A_n^2 \frac{\sigma_T^2}{\bar{T}^{-4}} \quad (37)$$

can be used in Eq. 33 to find C_n^2 . The values obtained for σ_n^2 using this approximation give satisfactory results in the prediction of centroid jitter when compared with experiments (D. Bruce, unpublished data).

When the turbulence is not yet fully developed, within a distance from the fire of four times the source radius, a separate method is used to calculate C_n^2 . This method, described elsewhere (Thompson and Devore, 1981), relates the variance of the temperature structure function, σ_T^2 , to the mean temperature gradients in the plume and assumes partial mixing of ambient air in this region. C_n^2 is calculated from Eq. 33, but Eq.'s 36 and 37 are replaced by

$$\sigma_T^2(D, r) = 3L_o^2 \frac{(\nabla T(D, r))^2}{1.91} \quad (38)$$

and

$$\sigma_n^2 = A_n^2 \left[\frac{\sigma_T^2}{(T_A T_M)^2} \right]. \quad (39)$$

In Eq. 39, T_M is the temperature of the partially mixed fractional volume of air. This method of calculation is invoked automatically by the model when the line of sight passes through the incompletely mixed region of the plume.

2.3 Model Implementation

2.3.1 FITTE: Fire Induced Transmittance and Turbulence Effects

FITTE performs calculations to predict effects for specific lines-of-sight. FITTE/FGLOW has three defined scenarios. The first two of these are the single line-of-sight (FITTE) scenarios that are used to predict the effects of the fire plume on general systems such as laser designators, and laser- or other seeker systems. Scenario three, discussed below as FGLOW, performs calculations for multiple lines of sight to predict radiant images of fires that may affect imaging systems such as IR cameras.

Scenarios one and two have identical geometry, as seen in Fig. 5, but differ in the direction of the turbulence calculation. Separate calculations are needed because calculation results depend upon path-weighted averages. The target and path radiance are calculated as seen from the observer position for both scenarios. For scenario 1, the turbulence effects are calculated at the 'target' position, that is for a laser beam propagating from observer to target, while for scenario 2 they are calculated at the 'observer' position, that is for a reflected laser beam propagating from target to observer.

2.3.1.1 Scenario 1

Scenario 1 corresponds most nearly to the original version of FITTE and it is the default for running the model. The "observer" can be any of the following: a laser designator, an observer with night vision goggles, a visible or IR imaging system. The "target" has no assigned physical dimensions but may have a non-ambient temperature and an emissivity. The radiative transfer calculations are performed so that the values produced are given at the observer position. The transmittance, of course, applies at either end of the path. Unless a waveband calculation is specified, turbulence effects parameters for the beam (which is assumed to be a laser beam) are predicted at the target position.

Various combinations of output parameters can be used to predict quantities such as the relative laser intensity on the target (initial intensity times transmittance divided by spot magnification), target contrast (target radiance divided by the sum of target and path radiances), etc.

2.3.1.2 Scenario 2

Scenario 2 is used in much the same way as scenario 1 and will perform the same calculations for radiative transfer. It was included for the calculation of turbulence effects on a laser beam reflected from the target to the observer. These effects will be different from those in scenario 1 for all cases when the fire plume is not at the center of the propagation path. This is because the turbulence in the plume distorts the wavefront in a manner similar to a set of diverging lenses so that the net effects depend on the path-weighted plume turbulence.

Time-series calculations can be performed for these scenarios to give tabular output of the parameters. Figure 6 shows graphs of the predicted fluctuations of several parameters.

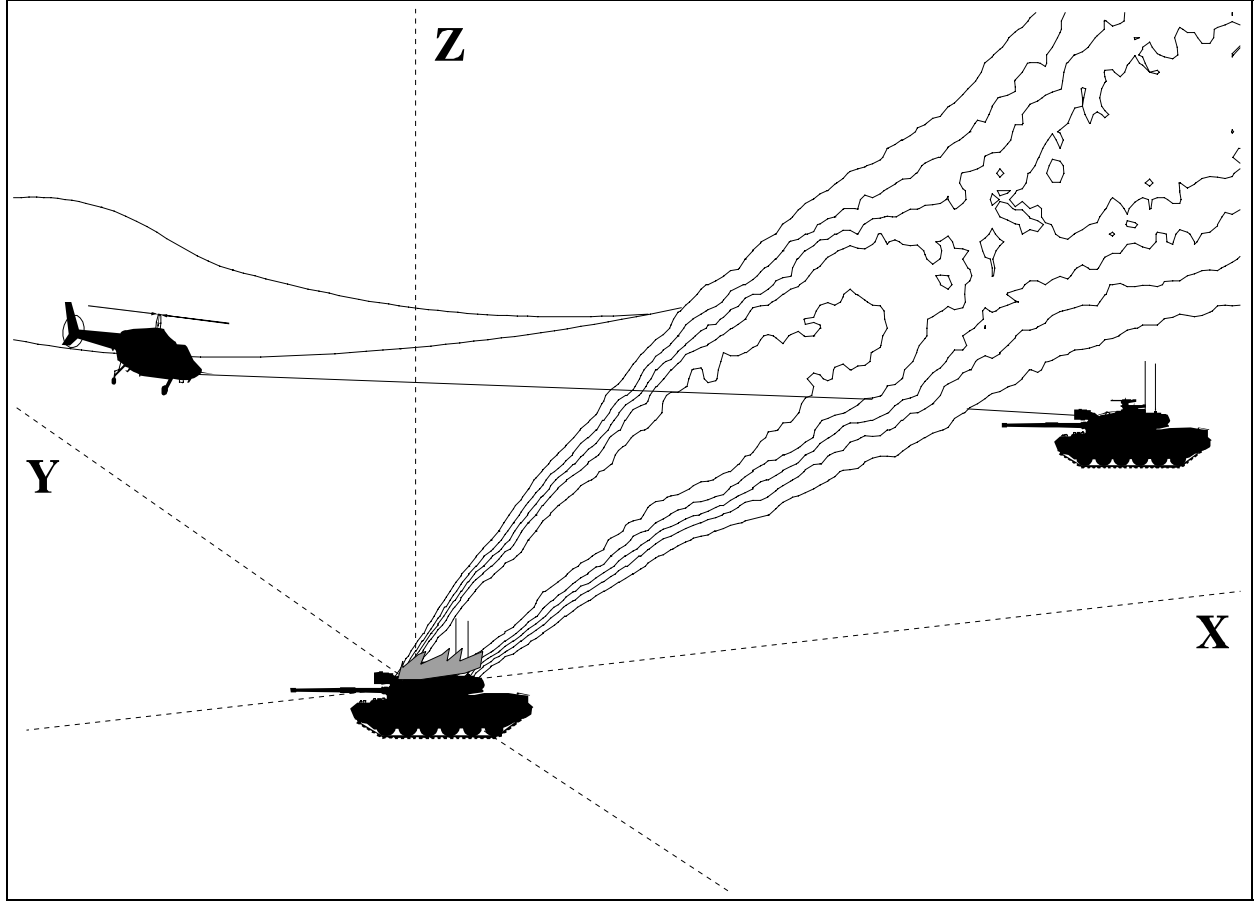


Figure 5. Geometry for the single line of sight scenarios. The helicopter would carry a laser designator for scenario 1 or a laser-guided munition for scenario 2.

2.3.1.3 Geometric Relations Used to Find Plume Parameters on the Line of Sight

Since integration along the LOS is required to evaluate the fire or plume effects, geometrical relations are needed to predict plume parameter values at points on the line-of-sight (LOS). The plume parameters are expressed as functions of the distance along the centerline and of the radial distance from the centerline to the point on the LOS.

Any point p on the LOS has a projection $(x_L, 0, z_L)$ on the plane of the time-averaged plume centerline, and the shortest distance from the centerline to the projected point is along a line perpendicular to the centerline. The equation of any such line has the form

$$z = mx + b, \quad (40)$$

where m is the negative inverse of the slope of the centerline at a point $(x_{CP}, 0, z_{CL})$, that is,

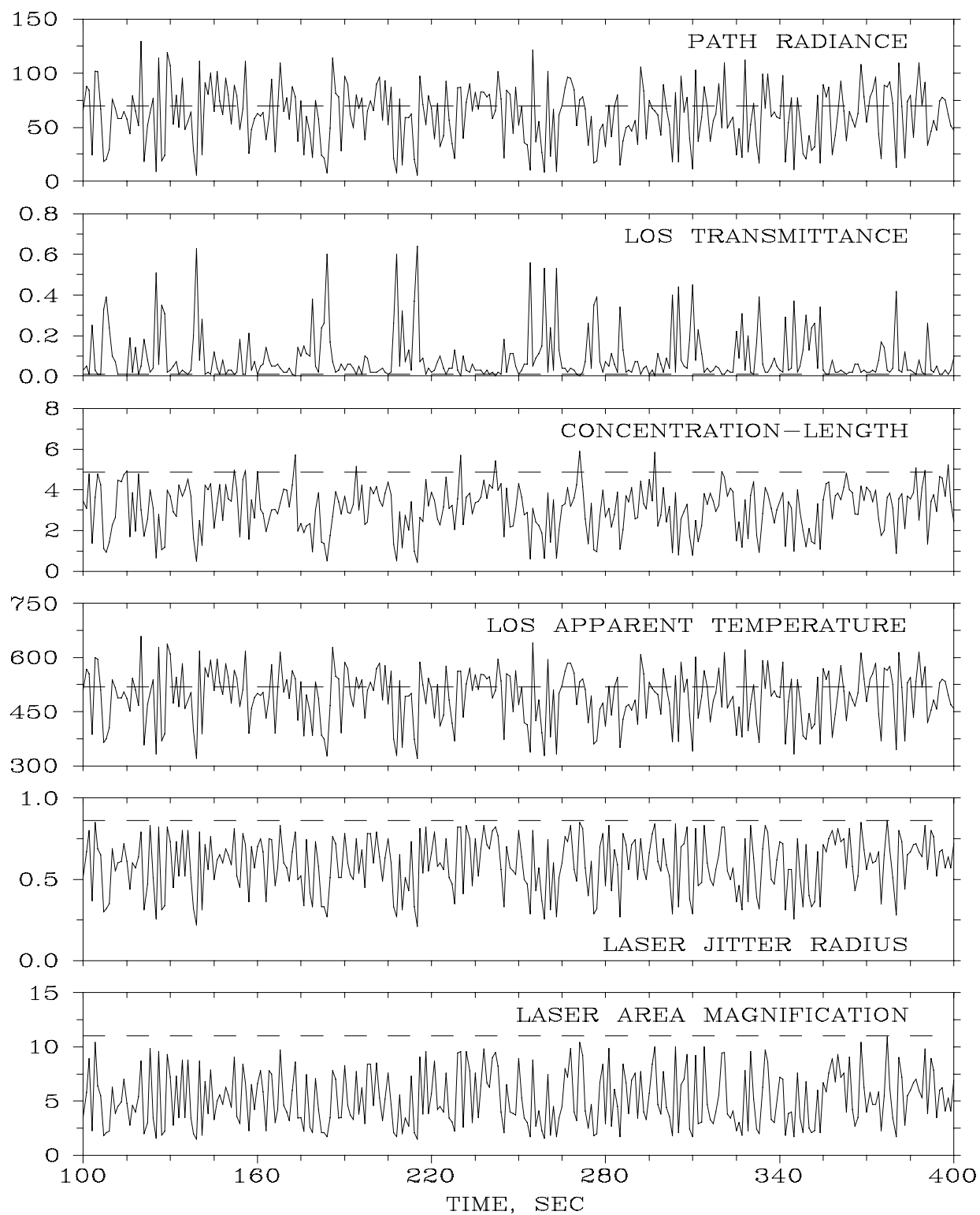


Figure 6. Graphs of model output data for a time-series calculation at 10.6 μm . The dashed lines show the values predicted by the mean-value model.

$$m = \left[-\frac{1}{dz/dx} \right] = -\frac{3}{2} \left(\frac{U}{C} \right)^{3/2} \sqrt{z_{CI} + z_V} . \quad (41)$$

Since $(x_L, 0, z_L)$ is also on the line, the intercept b is given by

$$b = z_L + \frac{3}{2} \left(\frac{U}{C} \right)^{3/2} \sqrt{z_{CI} + z_V} x_L . \quad (42)$$

An equation for z_{CI} , the centerline point closest to $(x_L, 0, z_L)$, is found by substituting Eq.'s **41** and **42** into Eq. **40** and replacing x_{CI} by substitution from the centerline equation. The equation obtained is

$$\frac{3}{2} \left(\frac{U}{C} \right)^3 (z_{CI} + z_V)^2 + (z_{CI} + z_V) - \frac{3}{2} (x_V + x_L) \left(\frac{U}{C} \right)^{3/2} \sqrt{z_{CI} + z_V} - z_V - z_L = 0 , \quad (43)$$

which can be solved by the substitution

$$Z = \sqrt{z_{CI} + z_V} , \quad (44)$$

and subsequent use of the solution for quartic equations found in the CRC© Handbook.

The distance of any point on the LOS from the closest centerline point can then be found and used to evaluate the plume parameters.

The distance from the centerline point to the projection of the LOS point on the x-z (wind-aligned) plane is denoted by h . The distance from the plume centerline to the ground along the same line is defined to be h_g . When h_g is greater than 2.0σ , the constants K_1 and K_2 in the plume equations are set to the values for a vertical plume, since no reflection from the ground will occur.

2.3.1.4 General Information about Calculations along the Line of Sight

For radiance and transmittance calculations, the default number of calculation intervals through the plume is 30, which gives a step length of 0.2 sigma. This does not affect the model accuracy for most lines of sight. Step size effects are most likely to occur for lines of sight near the plume centerline and very close to the fire. The calculation of turbulence effects is performed using an adaptive Simpson's rule integration subroutine, ASRI, rather than a fixed number of calculation intervals. A single calculation interval is used between the plume and the observer when molecular absorption calculations are performed.

When waveband calculations are performed, the molecular effects subroutines (the ATLESF set) are called for the first interval, and subsequent calls are made only when the temperature change from the previous interval exceeds a fraction of the previous value. The default for the fractional change is 0.10.

2.3.2 FGLOW: Fire/Fire Plume Radiant Emission and Transmittance

FGLOW is an extension of FITTE that performs calculations for multiple lines-of-sight to generate a simulated image matrix. It does not calculate turbulence effects on laser propagation.

Figure 7 shows scenario three, the FGLOW scenario. An imaging system is located at the observer position with its LOS specified by a "target" position, and a fire or a plume segment is within the field of view. FITTE calculates the path radiance for an array of "pseudo-target" positions to create a file that contains a matrix representation of the radiant image of the fire. The array is defined by an 'input card' to have n rows, m columns and an angular resolution (in milliradians) between elements.

Since the calculation matrix for the FGLOW calculations typically contains many lines of sight that do not pass through the plume, the model sets a flag and stores the values calculated for the first line of sight that does not intercept the plume. Calculation speed is increased by using these stored values for all subsequent lines of sight that do not intercept the plume.

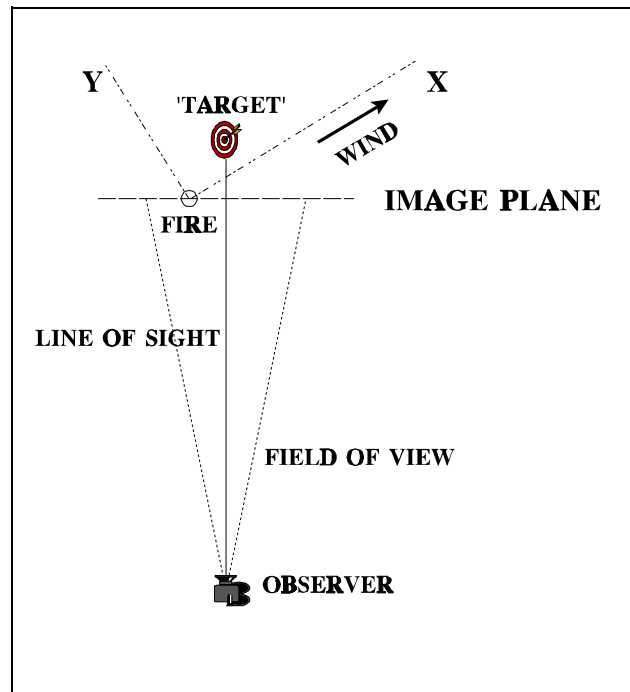


Figure 7. Top view of scenario 3 (FGLOW) geometry. Situation shown is for 240 degree wind direction of Example 9.

Chapter 3

Caveats

3.1 Grade of Software

The FITTE model should be classified as a research model. This choice of software grade is based on the fact that no quantitative evaluations have yet been made of the spatial and time variations that have been introduced into the model and to the limited evaluations of predictions of beam wander and beam spread.

3.2 Model Failure

The model will fail to run if selected input values do not meet acceptance criteria. Failure occurs if:

- (1) the observer and target positions are on the same side of the wind-aligned axis in the model coordinate system;
- (2) either waveband limit on the BAND card is outside the range of the molecular absorption data in BPARAM.DAT.

The model will fail to run if:

- (1) the files BPARAM.DAT and FIT4D.DAT are not located in the same directory as the executable program;
- (2) a non-EOSAEL format input card is encountered; or
- (3) an unexpected end-of-file is encountered in an input file.

The model will fail if you run out of disk space for the output files. This is most likely to happen if FGLOW is run for a large image matrix or a time-series of smaller FGLOW images.

3.2.1 Cautions

The model will run if many of the possible input parameters are out-of-bounds. In this case a default value will be substituted for the out-of-bound parameter, the output file will contain a message stating 'DEFAULT(S) REPLACE INVALID INPUT ON CARD *CARDNAME*' and the default value(s) will appear in the printout of input parameters contained in the output file.

Bounding values have been set for a parameter if the value is known to be physically bounded (e.g., target emissivity must be between 0 and 1) or if an out-of-bound value will affect the accuracy of model computations (windspeed must be greater than 0.10 since it appears in the denominator of several equations).

The model performance has been tested only under relatively benign atmospheric conditions: windspeeds less than about 10 m/s (22 mph), on clear or cloudy days with unstable or neutral stability. Model performance is expected to degrade under more severe weather conditions but it is not known how rapid or severe the degradation will be. There is currently no provision for including effects of obscurants such as rain, fog or smoke clouds along with those of the fire plume.

3.3 Verification Tests

Model verification has been obtained from laboratory and field tests. All comparisons to date have been made with the predictions of the time-averaged model. This is, actually, the most meaningful approach to the question of general model validity. Transmittance, radiance and plume centerline shape and spread for the time-averaged plume have all been shown to give good agreement with field test data. The laser wander and beam spread predictions were verified by laboratory experiments. Aerosol specific extinction gives generally good agreement with laboratory and field data, but visible and near-IR values of albedo are low compared to measured values.

Comparisons with field data suffer from various problems. If point measurements are made, the results depend strongly on plume meander due to changing wind conditions. If the instruments are at fixed positions it is possible that little or no data will be obtained. If data is obtained, auxiliary measurements are needed to determine the location of the probe within the plume relative to the instrument(s). If, as at the BICT III test, a crane is used to position an instrument cage within the plume, data will be obtained, but the data reduction problem of relative position is even more difficult. Similar problems occur for transmittance measurements that represent line-of-sight integrated data. As a result, limited data is available because of difficulties encountered both in making measurements through plumes in the field and in analysis of the data.

3.3.1 Fire and Plume Properties

The shape of the time-averaged plume centerline (Briggs, 1969) was based on extensive observations of plumes from smokestacks under a variety of meteorological conditions. The applicability of this model to ground-level small fires has been verified by comparing visible plume images (photographs or video) with model predictions for appropriate fire size and wind conditions. Good agreement has been reported (Bruce and Sutherland, 1986).

The plume centerline angle of elevation depends on the ratio of the vertical velocity to the (horizontal) windspeed. Plume angles of elevation as a function of windspeed have been reported (Hall and Manning, 1986) from imagery taken at BICT III. Digitized images from each of ten data segments were used in the analysis. The data segments were chosen to represent a range of windspeeds. After reclassifying the windspeed for two segments of the data, the authors found a linear relation between angle of elevation and windspeed for windspeeds ranging from 1 to 7 m/s. The authors mention that uncertainties are introduced in determining the position of the origin of the plume and the need to ignore centerline curvature.

Figure 8 shows the measured values compared with model predictions for the fire type closest to the BICT III fires. The error bars indicate the standard deviation of the data. Agreement is reasonable, but the difference in slope indicates that changes in the model would be appropriate. These should probably involve an increase in thermal flux as a function of windspeed. Experiments are currently being conducted to determine effects of windspeed on fire and plume parameters.

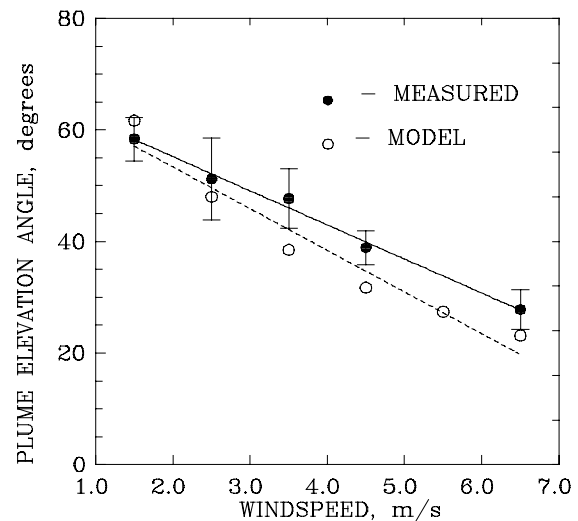


Figure 8. Comparison of measured and modeled plume elevation angles.

Another important measure for the plume model is how well it predicts plume spread. This can be verified by comparisons of total angular spread observed in images with the value obtained from the entrainment parameter, ξ , for various windspeeds. This type of comparison has been made for a number of plume images and, with the

assumption that the visible plume edge is at the 2σ point of the model Gaussian distribution, agreement is good. This means that the model predictions are typically within the range of uncertainty for the measured values.

3.3.2 Aerosol Optical Properties

Laboratory and field measurements of aerosol optical properties in plumes from diesel fuel fires have been reported. Figure 9 shows a comparison of extinction coefficients from FITTE with laboratory data. The laboratory measurements were made with a flow-through photoacoustical system with an incorporated short path transmissometer. Correlated measurements of aerosol characteristics were obtained by timed collection of filter samples and subsequent analyses to obtain total particle weight, particle size distribution and chemical identification. Error bars indicate variations of measured values with the naturally occurring variation of aerosol size distribution during a series of experiments. Agreement at $10.6\ \mu\text{m}$ is due to the fact that the measured values at that wavelength were those used to determine the absolute scale for the Mie calculations used for the model optical parameters at other wavelengths.

Two series of field measurements (Bruce and Richardson, 1983; Bruce et. al., 1989) of optical properties of diesel fire plume aerosols at $10.6\ \mu\text{m}$ gave extinction coefficients that averaged about 20% higher and that showed a greater variability. The authors attribute the increased values to the presence of a greater number of large aerosols in the measured size distributions. The values found from the field data (1.3 ± 0.7 and $1.2 \pm 0.3\ \text{m}^2/\text{g}$, respectively) overlap the laboratory value ($0.99 \pm 0.12\ \text{m}^2/\text{g}$).

The modeled and measured values of single scattering albedo are compared in Table 3. The measured values are from the same laboratory experiments as the specific extinction and are calculated using the formula $\omega = 1 - \alpha/\epsilon$. No value was obtained at $1.06\ \mu\text{m}$ because no gas that absorbs strongly at this wavelength is available to provide calibration data for the spectrophone and changes in beam geometry for different wavelengths preclude the use of calibration from other wavelengths (C. W. Bruce, private communication).

The substantial difference between the modeled and measured values at shorter wavelengths means that the values used in the model need to be revised. The revision awaits data at additional wavelengths that should be available in the near future (C. W. Bruce, private communication). The use of Mie calculations, which are valid only for spherical particles, and particle-to-void theory for the stringy aerosol particles is subject to large uncertainties, as was the assumption that the particles could be described by a bimodal size distribution. The primary effect on model output will be a change in predicted path radiance at visual and near-infrared wavelengths. Experimental runs using measured values, and with scaled increases in albedo values at intermediate wavelengths, indicate that path radiance will decrease by 12 to 15 percent in the visual and near-infrared wavelength regions.

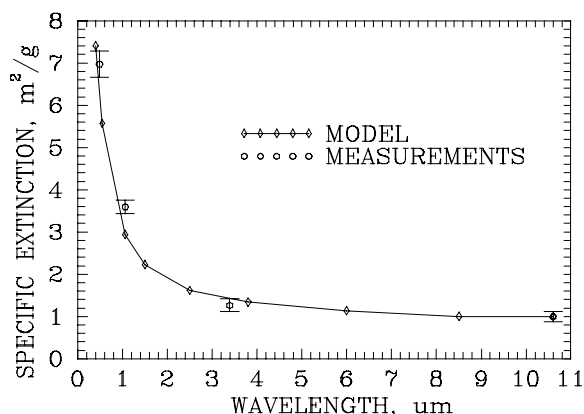


Figure 9. Comparison of measured (Bruce et. al., 1991) and modeled extinction coefficients.

Table 3. Comparison of Albedo Values

$\lambda\ (\mu\text{m})$	ω_{MODEL}	ω_{MEASURED}
0.488	0.25062	0.34720
3.390	0.22174	0.32540
10.600	0.15000	0.15000

3.3.3 Plume Distribution Functions

Radiant emission, measured with thermal imaging systems during the BEST ONE test, was used to check the predictions of FGLOW. Images were analysed to give the time dependence of the total area that exceeded various blackbody equivalent temperatures (S. B. Crow, private communication). Good agreement of measured and simulated radiation temperature spatial distributions was obtained for 'top hat' source temperatures ranging from 1223 to 1473 K (Bruce, 1989). This is roughly 300 K higher than the value currently used for the model. Peak temperatures measured close to the edge of one of the fuel drums during the BICT III test were approximately 1250 K (D. Bruce, unpublished data). Calibrated imagery taken at BEST ONE with short- and long-wavelength cameras and several narrow-band filters (Leidner and Clement, 1987) show maximum radiation temperatures between 800 and 1300 C for an open tray fire and between 600 and 900 C for burning vehicles where the flames were mostly enclosed.

Peak vertical plume velocities measured at the BICT III test (Bruce et. al., 1989) were approximately 2.9 m/s at 3 m from the fire and 1.2 m/s at about 14 m from the fire.

Molecular combustion product concentrations in diesel fire plumes have been measured (Bruce et. al., 1989; Kaaijk, 1986). Maximum measured carbon dioxide concentrations ranged from 100 ppm to >1000 ppm above the ambient concentration and the maximum measured water vapor increase ranged from 0 to 7 mbar above ambient. Other effluent gases occur in very low concentrations. Benzene was the prevalent aromatic hydrocarbon with a measured concentration range of 0.3 to 3.0 mg/m³ (Kaaijk, 1986), and carbon monoxide concentration was less than 100 ppm since it was not detected by the chemical analysis. The concentrations reported by Kaaijk represent an average value for the plume position during the sampling time, while those reported by Bruce et. al. include instantaneous as well as time-averaged values. The concentrations in both cases were measured approximately 15 m from the fire. The measurements can only be used as a check on whether the effluent concentrations used in FITTE are approximately correct.

The carbon dioxide concentration was chosen for comparison with the model because it is a more direct measurement. The assumption was made that the mean concentration at a distance of 15 m from the base of the plume was approximately 667 ppm. Data given for plume spread and fire size (Bruce et. al., 1989) were used to estimate values at the source and obtain a mean concentration of approximately 8000 ppm. This is much less than the 136000 ppm modeled in the earlier versions of FITTE. This very large number was obtained based on the assumption (Manning, 1985) that the effluent gases represented 100 percent of the gases above the fire and the fact that the effluent gas concentrations were not modeled as dependent on the burn rate. The current model for effluent gas concentrations ties their values to the rate of fuel consumption and results in source concentrations of carbon dioxide between 6000 and 17000 ppm, in satisfactory agreement with the measured values.

The aerosol mass concentrations reported from filter data (Kaaijk, 1986) ranged from 0.001 to 0.036 g/m³ and were not corrected for the time the sampler was not in the plume or for the fact that the sampling system was usually near the edge of the plume when it was within the plume. The time in the plume varied from less than 10 to 70 percent of the 20 minute sampling period. The peak aerosol mass concentrations derived from optical measurements within the plume (Bruce et. al., 1989) were typically 0.500 g/m³ with an observed maximum value greater than 0.640 g/m³. The same estimation procedure used for the source gaseous effluent concentration gives a source aerosol mean mass concentration of approximately 2.6 g/m³. This is about twenty percent higher than the value used in the model.

A less direct indicator of the adequacy of the plume distribution functions is given by comparison of measured and simulated transmittance. This comparison depends on accurate optical parameters as well as the distribution functions and must be performed with appropriate matching of beam parameters. Comparisons of measured transmittance at BEST ONE with FITTE predictions have been reported (Gillespie, 1987; Bruce, 1989). All of the results for this test are compromised by the fact that no survey data is available to provide reliable position data.

Gillespie used a modified version of FITTE (Manning, 1986) that was available in early 1987 with calculations from the PC version of LOWTRAN to account for transmittance effects of natural aerosols. This version of the model did not perform area averaging for large beam sizes. Trials were divided into two classes according to the magnitude of transmittance change during the trial. Results of comparing simulated single wavelength visible with measured broadband visible data were poor - results typically differed by more than 20%. Results at 1.06 μm were generally better - differences were within ten percent for five trials and greater than 20% for four. In the 3-5 μm band differences were less than 10% for five trials, less than 20% for three trials and greater than 20% for two trials. In the 8-14 μm band differences were less than 10% for two trials, less than 20% for three trials and greater than 20% for four trials. Gillespie categorizes these results as a fair validation of FITTE.

There are a number of factors that probably account for some of the disagreement. The measured transmittance at 1.06 μm is lower than that in the visible band for most of the tests used in the comparison. A later test (Farmer et. al., 1989) suggests that these results could have been caused by vignetting of the beam at one of the wavelengths, operation of a detector in a non-linear response range and/or misalignment of the optical system. For all wavelengths, there were a number of trials for which no comparison was made because the model indicated that the line of sight did not pass through the plume. This indicates problems with the available input data and may have affected all aspects of the comparison.

Bruce used the revised version of the 1987 FITTE module to perform comparisons for one of the BEST ONE trials. She varied the fire parameters to obtain good agreement with calibrated infrared imagery, and then used the area averaging feature of FGLOW (the angular resolution was chosen to match the transmissometer beam size) to find transmittance at three infrared wavelengths for a variety of positions in the plume. The area near the estimated position of the transmissometer line of sight was then examined, and an area was found in which agreement of simulation and measurements was less than 25% for all wavelengths.

3.3.4 Effects of Thermal Plume Turbulence on Laser Beam Propagation

Concurrent laboratory measurements have been made of temperature fluctuations in plumes and of laser beam spread and jitter for a beam traversing the plume (Bruce and Sutherland, 1986). These experiments verified the method used to calculate the localized turbulence structure function within the plume. The measured plume centerline temperature and radius were used to tailor the FITTE plume for simulations that showed that the FITTE predictions of laser beam wander are good (within 10%) and predictions of beam spread are good to satisfactory (within 15% to 25%) for regions outside the flames. The errors are greatest in the region just outside the flames. The experimental data identified a method of calculation to be used for the area close to the fire in which the plume is not yet well mixed.

Chapter 4

Operations Guide

FITTE can be run using the standard EOSAEL driver. It has also been furnished with a dedicated driver for use on a personal computer. If this driver is to be used, the FITTE subroutines should be linked with the program FITDRV.FOR that is found in the FITACC directory. FITDRV.FOR contains several subroutines and a block data file EOSLBD. Several example auxiliary programs are furnished that can be used to create pseudo-greyscale printouts of FGLow output or to modify the FGLow output files for use by programs that can create contour plots. These examples are described in Appendix A.

4.1 Input

The input cards use the standard EOSAEL format (A4, 6X, 7E10.4). Repeated scenarios can be run with the usual EOSAEL procedure. Six to nine data cards are normally used, with GO and DONE cards used to control program execution. Tables 4-17 contain descriptions of the FITTE input cards. Additional information about some of the cards is given in the accompanying text. There are new cards defined and changes to some previously defined cards.

If the module is run with the standard EOSAEL driver an EOSAEL WAVL card is required, as is a card to call the FITTE module. Usually the cards REFD, SCEN, SRCL, METD and either DETD or SCN3 are required. SCEN and METD may be omitted if the data was furnished to EOSAEL main. In that case flags, used as FITTE calling parameters, indicate the need to convert the data units. All other cards are used to invoke various model options.

Table 4. The REFD Card

Identifier	Variable	Default	Description
REFD			Reference data
	XHEAD		x-axis heading of user coordinate system (degrees clockwise from north)
	ITYPE	1	code for fire type (1 - 4)
	ISCN	1	code to specify FITTE scenario (1 - 3)
	IAVG	0	code to chose time-averaged plume calculation: 0 or positive number \Rightarrow use 4-D plume negative number \Rightarrow use time-averaged plume
	NTURB	0	negative value cancels turbulence calculations

REFD contains information about the orientation of the user coordinate system and several model control parameters. The position data for the observer and target, given on the SCEN card, and for the fire, given on the SRCL card,

can be in any convenient right-handed coordinate system. The x-axis heading of that (user) coordinate system must be given. This heading and the wind direction on the METD card are given by angles measured clockwise from north. The control parameters on REFD are used as indicated.

Table 5. The SCEN Card

Identifier	Variable	Default	Description
SCEN	Line of sight data		
	UO(1)		observer x coordinate (m)
	UO(2)		observer y coordinate (m)
	UO(3)		observer z coordinate (m)
	UT(1)		target x coordinate (m)
	UT(2)		target y coordinate (m)
	UT(3)		target z coordinate (m)

The SCEN card gives the observer and target positions in the user coordinate system. These positions must lie on opposite sides of the x-axis in the FITTE coordinate system. The origin of the FITTE coordinate system is at the position in the user coordinate system given on the SRCL card. The x-axis of the FITTE coordinate system is aligned with the wind vector.

Table 6. The SRCL Card

Identifier	Variable	Default	Description
SRCL	Fire location data		
	US(1)		x-coordinate of the center of the fire (m)
	US(2)		y-coordinate of the center of the fire (m)
	US(3)		z-coordinate of base of fire (m)

Most of the input data for the METD card is self-explanatory. The wind direction is determined by the usual meteorological convention, i.e., the upwind direction measured clockwise from north. The Pasquill stability category has a range of 1 to 6. Compared with the usual classification 1 = A, 2 = B, etc.

Table 7. The METD Card

Identifier	Variable	Default	Description
METD			Meteorological data
	UBAR		mean ambient windspeed (m/s)
	WDIR		wind direction (meteorological convention, degrees)
	TAIR		ambient air temperature (Celsius)
	RH		relative humidity (percent)
	RHO		ambient air density (g/m ³)
	IPAS		Pasquill stability category (range is 1 to 6)

The DETD card is used to specify the initial laser beam diameter for a scenario 1 or 2 simulation.

Table 8. The DETD Card

Identifier	Variable	Default	Description
DETD			Laser data
	BEAM		beam diameter (cm)

The TARG card is used to obtain contrast data for a target with a temperature other than ambient for a scenario 1 or 2 situation.

Table 9. The TARG Card

Identifier	Variable	Default	Description
TARG			Target data for thermal emission calculations
	TTARG		target temperature (Celsius)
	ETARG		target emissivity (dimensionless, range 0 to 1)

The MOLS card is used to specify inclusion of molecular effects in the radiance and transmittance calculations. It also controls whether the transmittance and radiance calculations are performed only through the plume, or if the effect of molecular absorption and emission in the atmosphere between plume and observer is included. The ambient carbon dioxide and water vapor concentrations are used in this calculation; other atmospheric gases are not included. If IATM is 1, the stepwise calculation through the plume is continued from the near plume edge to the observer position.

Table 10. The MOLS Card

Identifier	Variable	Default	Description
MOLS			Molecular effects calculation control
	IMOL	1	flag for molecular transmittance calculation: 0 \Rightarrow molecular transmittance not included 1 \Rightarrow molecular transmittance is included
	IATM	0	flag for calculations outside the plume: 0 \Rightarrow omit calculations between observer and plume 1 \Rightarrow include calculations between observer and plume

Table 11. The BAND Card

Identifier	Variable	Default	Description
BAND			Waveband calculation control
	IBAND	0	flag waveband calculations: 0 \Rightarrow single wavelength calculation 1 \Rightarrow perform waveband calculation
	WVN1		beginning wavenumber of band (cm^{-1})
	WVN2		ending wavenumber of band (cm^{-1})
	NWVN	1	number of wavenumber intervals in band (must be odd)
	IRESP	0	instrument response function over waveband: 0 - rectangular 1 - triangular 2 - trapezoidal
	IPSPEC	0	Switch printing of spectrally resolved values 0 \Rightarrow do not print resolved values 1 \Rightarrow print resolved transmittance and radiance values

The BAND card is used to specify waveband calculations and to furnish parameters for their control. It also controls the instrument response function used for a waveband calculation. There are three instrument response functions from which the user may choose: a rectangle, a triangle, and a trapezoid. The code in subroutine RESPNS is written so that other functions may be added easily and the method for constructing instrument response functions is described in the source code. When a waveband calculation is performed for the FGLOW scenario the aerosol optical properties used are those for the center wavelength of the band. If the FGLOW output data is specified as apparent temperature, a blackbody equivalent temperature is calculated based on a conversion of the band-integrated radiation to a weighted average value at the center wavelength of the band.

The beginning and ending wavenumbers of the band and the number of calculation points in the band are specified by the user. The response function value is then calculated for each of the points. The rectangle has values of one in the band, zero outside the band, and 0.5 at the boundaries. The triangle has a peak of one and goes to zero at the boundaries. The trapezoid is zero at the boundaries, rises linearly from zero to one over the outer 20% of the band on each side, and has a value of one for the central 60% of the band.

The number of calculation points in the band must be odd so that a point is defined at the center of the band. The code checks for this and corrects it if necessary. If such a correction is made, the number of points (and therefore the wavenumber increment) will differ from the user input.

Table 12. The OPT1 Card

Identifier	Variable	Default	Description
OPT1			Optional parameters for calculation control
	TCRITA	0.10	Fractional change in temperature which triggers a call to the band model
	NUMINT	30	Number of calculation steps through the plume
	NUMSEG	1	Number of path segments for calculation from plume to observer

The OPT1 card permits the user to override the default values of TCRITA, the fractional change in temperature that triggers calls to ATLESF, NUMINT, the number of calculation intervals through the plume (which should be an even number), and NUMSEG, the number of calculation intervals between the plume and observer. The default values have been found to speed calculations and still give good results.

The SCN3 card supplies imager parameters needed for scenario 3 calculations and control. Note that although the option to produce apparent temperature output image data files has not been removed from the code, it is suggested that this option should not be used. Accessory programs, described in Appendix A, can be used to transform the radiance image data to apparent temperature image data.

Table 13. The SCN3 Card

Identifier	Variable	Default	Description
SCN3			Imager parameters for scenario 3 (FGLOW)
	AINC		resolution per pixel (milliradians)
	NGX		number of columns of pixels
	NGZ		number of rows of pixels
	IAPT	0	code for type of data stored: 0 ⇒ radiance and transmittance data 1 ⇒ apparent temperature data

Table 14. The TCAL Card

Identifier	Variable	Default	Description
TCAL			Time-series calculation control
	STIME	100	start time for calculations (seconds after start of fire)
	TINC	1	time increment between calculations (s)
	NCALC	1	number of calculations in time series
	VELO	0	velocity of observer toward target along LOS (m/s)

The TCAL card is used to specify an internal time-series calculation. If FITTE is called by other modules within EOSAEL, only the output parameters from the final time will be passed back to the calling routine. Time-series calculations will suppress printing of waveband resolved output. All times will be converted to integers because the built in time constant for calculations is 1 second. The VELO parameter is normally zero, but it can be used to specify movement of the observer toward the target along the LOS during the time series calculation. **Note** that if the observer crosses the model system wind-aligned axis the calculations will be aborted and a message will be written to the output file.

The SVAR card lets the user modify certain fire parameters. It is intended primarily to permit matching of parameters for comparison with experimental data. **THIS CARD SHOULD BE USED WITH CAUTION - IT CAN CAUSE UNREALISTIC COMBINATIONS OF FIRE PARAMETERS AND ERRONEOUS PREDICTIONS.** The user should monitor the value of vertical wind, W_o , printed in the output file when the fire parameters are varied. A value much outside the range 1.5 - 3 m/s indicates that the combined fire parameters have changed significantly from measured values and the model predictions may not be accurate. See Appendix D for a discussion of varying the fire parameters and developing model fire parameters from data.

Table 15. The SVAR Card

Identifier	Variable	Default	Description
SVAR			Variation of fire parameters
	TEMPIN	973.16	fire mean temperature (K)
	EFFAC	1	fractional multiplier of aerosol efficiency factor
	RADIN		radius of fire (m)
	BTIME	1500	burn time (s)

The mean fire temperature, TEMPIN, can be varied fairly freely. The current value seems to give accurate radiation temperature distributions for fires enclosed within metallic hulls. For open burning of fuel the appropriate mean temperature may be several hundred degrees higher. If the variation of the fire parameters is performed to match experimental data, the peak temperature in the Gaussian plume at the fire will be roughly 2.9 times the mean temperature used here.

EFFAC is a fractional multiplier that allows the user to vary the creation of smoke aerosols. It should normally be set to 1.0, but can be any number. Values between about 0.67 and 1.33 would cover the general range of smoke variation for hydrocarbon fuel fires.

RADIN allows the user to vary the fire radius. Plume scaling in the atmosphere is generally considered to occur for fire diameters of no less than 1 meter, so the minimum value for RADIN should be 0.5 m. **Note** that the actual fire image will appear to have approximately 2/3 the specified source radius.

BTIME allows the user to vary the total burn time for the fire. The current value is 1500 seconds (25 min). Large variations from this value would be inappropriate for open burning conditions, but substantial increases might be called for to simulate an enclosed fire where the burn rate is controlled by an inadequate oxygen supply.

The GO card is used to indicate that repetitive calculations are to be performed for which new parameter values are read between model runs.

Table 16. The GO Card

Identifier	Variable	Default	Description
GO			Execute and read data for a subsequent run

Table 17. The DONE Card

Identifier	Variable	Default	Description
DONE			Execute and return control to EOEXEC

The default values shown on the cards are those used if no value is furnished. As can be seen, not all variables have default values. There are other (default substitute) values used when certain input parameters are outside an appropriate range of values. A notice that identifies the input card involved is printed in the output file if any substitution of values is made.

Selecting a turbulence effects calculation, a time series calculation or a scenario 3 (FGLOW) calculation (particularly for waveband calculations) may increase run time significantly. Typical run times on a 20 Mhz 386 PC with coprocessor are shown in Table 18.

Table 18. Run times for selected run conditions

Single LOS	Single wavelength	1 min 12 sec
Single LOS	25 Wavenumber band	0 min 13 sec
Single LOS 25 point time series	Single wavelength with turbulence effects without turbulence effects	14 min 23 sec 0 min 34 sec
Single LOS 25 point time series	25 Wavenumber band	1 min 2 sec
25 by 25 array (625 total LOS)	Single wavelength	3 min 45 sec
25 by 25 array (625 total LOS)	25 Wavenumber band	39 min 28 sec

4.2 Output

4.2.1 Parameters Returned to the Calling Routine

The parameters returned to the calling routine have been increased. They now include the following:

FITRAN - the total transmittance for the line-of-sight,
 IERR - a code to indicate an invalid input card identifier,
 ATRAD - the attenuated target radiance for the line-of-sight,
 PATRAD - the path radiance for the line-of-sight,
 CONLEN - the aerosol concentration-length product,
 SPTMAG - the turbulence-induced spot (area) magnification, and
 JITRAD - the turbulence-induced beam wander radius.

All of the parameters (except the error code) are output for scenario 1 or 2 calculations that include turbulence effects. If turbulence effects calculations are omitted the last two parameter values are meaningless.

For FGLOW calculations, the output parameters are those for the LOS with the highest path radiance.

4.2.2 Output Printed or Stored in Files

FITTE scenario 1 or 2 output is contained in a single file. Samples are shown in the example section. Most of the input data are listed, plume parameters are given for the calculation point on the LOS that is closest to the plume centerline, and the model predictions are printed. The output parameters provided are the modeled calculation time, total transmittance, aerosol transmittance, attenuated target radiance, path radiance, 'apparent temperature', the concentration-length, and, for single wavelength calculations that include turbulence effects, the laser spot magnification and jitter radius.

If transmittance and radiance are calculated over a spectral band, the user has the option (set IPSPEC = 1 on BAND) of printing the spectrally resolved values of the radiative transfer predictions. Quantities printed are the wavelength, wavenumber, transmittance, target radiance, path radiance, total radiance, and instrument spectral response. This option cannot be exercised if a time-series or an FGLOW calculation is being performed.

For the FGLOW scenario, two output files are created. The standard output file contains a summary of input data and information about the matrix data file created. The second file created contains a header with information on calculation parameters and ngx times ngz rows that contain either path radiance and total transmittance data or apparent temperature data for the image matrix specified on the SCN3 card. Samples are shown in the examples. This output file is named FGLOW1.FDT for a single image calculation. If a time series of n images is calculated the files will be named FGLOW1.FDT to FGLOWn.FDT. The FGLOW data file(s) should be renamed if you wish to keep them, since the model will overwrite one (or more) of the file(s) the next time it is run.

Chapter 5

Sample Runs

This section shows examples for running FITTE for various conditions. The examples show the input card file, the output file, and may be accompanied by comments, an FGLOW data file and/or illustrations of FGLOW output.

The examples were chosen to illustrate use of most of the model options.

Notes:

- (1) The examples were all run with the synthetic wind fluctuation file FITEX.DAT copied to FIT4D.DAT. To obtain more realistic output, one of the wind fluctuation files based on field data (see information in the file README.FIT) should be copied to FIT4D.DAT after the examples are run.
- (2) The input files listed are those for use with the PC version of the code using FITDRV as the main program. Several additional cards are needed to use the EOSAEL main driver. These include a WAVL and a FITTE card as a minimum, and may include cards with climate and geometry data.
- (3) The EOSAEL header page has been omitted from the output files.
- (4) The DONE, END and STOP cards have been omitted from most of the examples.

5.1 Example 1: A scenario 1 calculation for a single wavelength

The user coordinate system positive x-axis points east, a type 2 fire is used for a scenario 1 calculation through a '4-D' plume. The target temperature is 10 C and it has an emissivity of 0.8. The initial laser beam diameter is 0.3 cm.

```

INPUT:  REFD      90.0      2.      1.      1.
        SCEN      8.0     -100.0     6.0      8.0     900.0     6.0
        DETD      0.30
        METD      3.0      270.      6.5      83.0     1200.0     3.0
        SRCD      0.0      0.0      0.0
        TARG      10.      0.8
        DONE
        END
        STOP

OUTPUT:

*****
*   EOSAEL 92   *
*  4D FITTE INPUT  *
*****

FIRE TYPE: TRUCK

X-AXIS HEADING:    90.0 DEG CW FROM NORTH

POSITION M (      X      ,      Y      ,      Z      ) :
OBSERVER (      8.0,    -100.0,      6.0 )
TARGET   (      8.0,     900.0,      6.0 )
FIRE     (      0.0,      0.0,      0.0 )

METEOROLOGICAL DATA :
WINDSPEED      3.0 M/S      WIND DIRECTION    270.0 DEG
TEMPERATURE     6.5 C      RELATIVE HUMIDITY  83.0 %
AIR DENSITY    1200.0 G/M**3  PASQUILL CATEGORY  3

TARGET TEMPERATURE  10.0 C      EMISSIVITY    0.80

LASER WAVELENGTH    0.63 UM      BEAM DIAMETER  0.30 CM

PLUME CONSTANTS :
VERTICAL WIND (W0)   2.39 M/S      COEFFICIENT (C)      6.906
BUOYANCY FLUX (F)   37.5      VIRTUAL SOURCE POSITION (M)
ENTRAINMENT CONSTANT 0.4134      XV:    -7.12,  ZV:    -8.52

PLUME-LOS GEOMETRIC AND DISTRIBUTION FUNCTION DATA AT CLOSEST APPROACH:

CENTERLINE COORDINATES (      7.26,    -0.12,     5.68 ) M
LOS COORDINATES (      8.00,    -0.24,     6.00 ) M
DISTANCE      0.82 M      EXCESS TEMPERATURE    153. C
PLUME RADIUS   2.32 M      AEROSOL DENSITY      0.25 G/M**3

*****
*   4D FITTE PREDICTIONS   *
*****

TIME  TRANSMITTANCE  ATTENUATED  SPOT  JITTER
sec   TOTAL  AEROSOL  TARG RAD  PATH RAD  APP TEMP  CL  MAGN  RADIUS
      w/m**2/sr/um  kelvin  g/m**2  m
-----
100.  0.00   0.00   0.129E-28  0.275E-15  403.0   1.25  11.6  0.00

```

5.2 Example 2: A scenario 2 calculation for a single wavelength

The only change from example 1 is that the calculation is done for scenario 2. Note the effect of reversing the direction of the calculation on the turbulence effects output.

```

INPUT:  REFD      90.0      2.      2.      1.
        SCEN      8.0     -100.0     6.0      8.0     900.0     6.0
        DETD      0.30
        METD      3.0      270.      6.5      83.0     1200.0     3.0
        SRCD      0.0      0.0      0.0
        TARG      10.      0.8

OUTPUT:

*****
*   EOSAEL 92   *
* 4D FITTE INPUT *
*****

FIRE TYPE: TRUCK

X-AXIS HEADING:  90.0 DEG CW FROM NORTH

POSITION M (   X   ,   Y   ,   Z   ) :
OBSERVER   (   8.0 , -100.0 ,   6.0 )
TARGET     (   8.0 ,  900.0 ,   6.0 )
FIRE       (   0.0 ,   0.0 ,   0.0 )

METEOROLOGICAL DATA :
WINDSPEED      3.0 M/S      WIND DIRECTION      270.0 DEG
TEMPERATURE     6.5 C      RELATIVE HUMIDITY     83.0 %
AIR DENSITY     1200.0 G/M**3  PASQUILL CATEGORY  3

TARGET TEMPERATURE  10.0 C      EMISSIVITY      0.80

LASER WAVELENGTH  0.63 UM      BEAM DIAMETER    0.30 CM

PLUME CONSTANTS :
VERTICAL WIND (W0)  2.39 M/S      COEFFICIENT (C)      6.906
BUOYANCY FLUX (F)  37.5          VIRTUAL SOURCE POSITION (M)
ENTRAINMENT CONSTANT  0.4134      XV:  -7.12, ZV:  -8.52

PLUME-LOS GEOMETRIC AND DISTRIBUTION FUNCTION DATA AT CLOSEST APPROACH:

CENTERLINE COORDINATES (   7.26,  -0.12,   5.68 ) M
LOS COORDINATES      (   8.00,  -0.24,   6.00 ) M
DISTANCE             0.82 M      EXCESS TEMPERATURE    153. C
PLUME RADIUS         2.32 M      AEROSOL DENSITY      0.25 G/M**3

*****
*   4D FITTE PREDICTIONS   *
*****

TIME  TRANSMITTANCE  ATTENUATED  SPOT  JITTER
sec   TOTAL  AEROSOL  TARG RAD  PATH RAD  APP TEMP  CL  MAGN  RADIUS
      watts/m**2/sr/um  kelvin  g/m**2  m
100.  0.00  0.00  0.129E-28  0.275E-15  403.0  1.25  1.0  0.00

```

5.3 Example 3: A scenario 1 calculation for a (visible) waveband

Note that you are notified that FITTE does not include molecular effects for this waveband.

```

INPUT:  REFD      90.0      2.      1.      1.
        SCEN      8.0      -100.0    6.0      8.0      900.0      6.0
        DETD      0.30
        METD      3.0      270.      6.5      83.0      1200.0      3.0
        SRCD      0.0      0.0      0.0
        TARG      10.      0.8
        BAND      1.      13000.    19231.    25.      2.      0.

OUTPUT:

*****
*   EOSAEL 92   *
* 4D FITTE INPUT *
*****

FIRE TYPE: TRUCK

X-AXIS HEADING:  90.0 DEG CW FROM NORTH

POSITION M (   X   ,   Y   ,   Z   ) :
OBSERVER   (   8.0 , -100.0 ,   6.0 )
TARGET     (   8.0 ,  900.0 ,   6.0 )
FIRE       (   0.0 ,   0.0 ,   0.0 )

METEOROLOGICAL DATA :
WINDSPEED      3.0 M/S      WIND DIRECTION      270.0 DEG
TEMPERATURE     6.5 C      RELATIVE HUMIDITY     83.0 %
AIR DENSITY     1200.0 G/M**3  PASQUILL CATEGORY 3

TARGET TEMPERATURE 10.0 C      EMISSIVITY      0.80

WAVEBAND DATA :
WAVEBAND FROM 13000.00 CM-1 TO 19231.00 CM-1      CENTER WAVELENGTH 0.621 UM
25 POINTS RESOLUTION      INSTRUMENT RESPONSE: TRAP      MOLECULES INCLUDED: YES
WAVEBAND DOES NOT OVERLAP FITTE MOLECULAR DATA

PLUME CONSTANTS :
VERTICAL WIND (W0)      2.39 M/S      COEFFICIENT (C)      6.906
BUOYANCY FLUX (F)      37.5      VIRTUAL SOURCE POSITION (M)
ENTRAINMENT CONSTANT   0.4134      XV: -7.12, ZV: -8.52

PLUME-LOS GEOMETRIC AND DISTRIBUTION FUNCTION DATA AT CLOSEST APPROACH:

CENTERLINE COORDINATES (   7.26,  -0.12,   5.68 ) M
LOS COORDINATES      (   8.00,  -0.24,   6.00 ) M
DISTANCE             0.82 M      EXCESS TEMPERATURE      153. C
PLUME RADIUS         2.32 M      AEROSOL DENSITY      0.25 G/M**3

*****
*   4D FITTE PREDICTIONS   *
*****

TIME      TRANSMITTANCE      ATTENUATED
sec      TOTAL  AEROSOL      TARG RAD  PATH RAD      APP TEMP      CL
                                watts/m**2/sr      kelvin      g/m**2

100.      0.00      0.00      0.283E-36      0.860E-14      448.5      1.25

```

5.4 Example 4: A scenario 1 time-series calculation for a single wavelength

The TCAL card is used to specify a time-series calculation. The calculation starts at 100 seconds after the start of the fire. The interval between calculations is 1 second, and 11 calculations are performed to span a ten second period. Note that, at this wavelength (1.06 μm), the inclusion of molecular absorption has no effect on the transmittance.

```

INPUT:  REFD      90.000      3.000      1.      1.
        SCEN      5.000     400.000      3.00     5.000   -800.000      3.0
        SRCD      0.000      0.000      0.000
        DETD      5.000
        TARG      37.0        1.0
        METD      4.000     270.000     27.000     60.000   1009.728      4.000
        TCAL      100.       1.        11.        0.
        MOLS      1.         1.

```

OUTPUT:

```

*****
*   EOSAEL 92   *
* 4D FITTE INPUT *
*****

FIRE TYPE: TANK

X-AXIS HEADING:      90.0 DEG CW FROM NORTH

POSITION M (      X      ,      Y      ,      Z      ) :
OBSERVER (      5.0,     400.0,      3.0 )
TARGET   (      5.0,    -800.0,      3.0 )
FIRE     (      0.0,      0.0,      0.0 )

METEOROLOGICAL DATA :
WINDSPEED      4.0 M/S      WIND DIRECTION      270.0 DEG
TEMPERATURE     27.0 C      RELATIVE HUMIDITY    60.0 %
AIR DENSITY    1009.7 G/M**3  PASQUILL CATEGORY  4

TARGET TEMPERATURE  37.0 C      EMISSIVITY      1.00

LASER WAVELENGTH   1.06 UM      BEAM DIAMETER    5.00 CM

PLUME CONSTANTS :
VERTICAL WIND (W0)  2.78 M/S      COEFFICIENT (C)      10.887
BUOYANCY FLUX (F)  169.1         VIRTUAL SOURCE POSITION (M)
ENTRAINMENT CONSTANT  0.4433     XV: -17.71, ZV: -18.49

PLUME-LOS GEOMETRIC AND DISTRIBUTION FUNCTION DATA AT CLOSEST APPROACH:

CENTERLINE COORDINATES (      3.87,     -0.52,      3.24 ) M
LOS COORDINATES (      5.00,     -0.50,      3.00 ) M
DISTANCE      1.15 M      EXCESS TEMPERATURE      0. C
PLUME RADIUS   2.87 M      AEROSOL DENSITY      1.28 G/M**3

```

 * 4D FITTE PREDICTIONS *

FITTE OUTPUT FOR TIME-SERIES CALCULATION

TIME sec	TRANSMITTANCE		ATTENUATED		APP TEMP kelvin	CL g/m**2	SPOT MAGN	JITTER RADIUS m
	TOTAL	AEROSOL	TARG RAD watts/m**2/sr/um	PATH RAD				
100.	0.00	0.00	0.107E-14	0.296E-01	622.6	3.05	172.4	0.44
101.	0.00	0.00	0.446E-14	0.321E+01	792.9	2.56	224.9	0.49
102.	0.00	0.00	0.317E-17	0.157E+00	674.2	5.03	477.0	0.66
103.	0.00	0.00	0.278E-13	0.134E-03	499.1	1.94	80.6	0.32
104.	0.00	0.00	0.250E-15	0.304E+00	697.0	3.54	539.4	0.69
105.	0.00	0.00	0.832E-15	0.596E+00	721.9	3.14	327.5	0.56
106.	0.00	0.00	0.171E-15	0.707E-01	648.5	3.67	291.5	0.54
107.	0.05	0.05	0.409E-12	0.148E-04	461.8	1.03	49.6	0.26
108.	0.06	0.06	0.530E-12	0.159E-04	462.9	0.94	61.6	0.29
109.	0.03	0.03	0.240E-12	0.688E-03	531.1	1.21	70.9	0.30
110.	0.00	0.00	0.727E-14	0.865E+00	736.5	2.40	340.0	0.57

5.5 Example 5: A scenario 1 calculation with variation of fire parameters and with printout of spectrally resolved results for a selected instrument response function

This calculation is performed over an infrared waveband. The last two parameters on the BAND card specify use of a trapezoidal response function and printout of spectrally resolved output. Note the use of the SVAR card to specify a higher fire temperature.

INPUT:	REFD	90.0	2.	1.	1.		
	SCEN	0.0	0.0	80.0	30.0	1800.0	20.0
	DETD	0.30					
	METD	3.0	255.	6.5	83.0	1200.0	3.0
	SRCD	-6.0	1650.0	0.0			
	TARG	10.	0.8				
	SVAR	1223.	1.				
	BAND	1.	2600.	3300.	25.	2.	1.

OUTPUT: (see next two pages)

```

*****
*   EOSAEL 92   *
* 4D FITTE INPUT *
*****

FIRE TYPE: TRUCK
USER ENTERED FIRE VARIATION:
AVERAGE TEMPERATURE: 1223. K

X-AXIS HEADING: 90.0 DEG CW FROM NORTH

POSITION M ( X , Y , Z ) :
OBSERVER ( 0.0, 0.0, 80.0 )
TARGET ( 30.0, 1800.0, 20.0 )
FIRE ( -6.0, 1650.0, 0.0 )

METEOROLOGICAL DATA :
WINDSPEED 3.0 M/S WIND DIRECTION 255.0 DEG
TEMPERATURE 6.5 C RELATIVE HUMIDITY 83.0 %
AIR DENSITY 1200.0 G/M**3 PASQUILL CATEGORY 3

TARGET TEMPERATURE 10.0 C EMISSIVITY 0.80

WAVEBAND DATA :
WAVEBAND FROM 2600.00 CM-1 TO 3300.00 CM-1 CENTER WAVELENGTH 3.390 UM
25 POINTS RESOLUTION INSTRUMENT RESPONSE: TRAP MOLECULES INCLUDED: YES

PLUME CONSTANTS :
VERTICAL WIND (W0) 2.16 M/S COEFFICIENT (C) 6.666
BUOYANCY FLUX (F) 37.5 VIRTUAL SOURCE POSITION (M)
ENTRAINMENT CONSTANT 0.4359 XV: -8.68, ZV: -9.38

PLUME-LOS GEOMETRIC AND DISTRIBUTION FUNCTION DATA AT CLOSEST APPROACH:

CENTERLINE COORDINATES ( 25.81, 1657.55, 19.09 ) M
LOS COORDINATES ( 27.65, 1659.16, 24.69 ) M
DISTANCE 6.12 M EXCESS TEMPERATURE 0. C
PLUME RADIUS 7.24 M AEROSOL DENSITY 0.00 G/M**3

*****
* 4D FITTE PREDICTIONS *
*****

TIME TRANSMITTANCE ATTENUATED
sec TOTAL AEROSOL TARG RAD PATH RAD APP TEMP CL
g/m**2
100. 0.85 0.85 0.105E-01 0.714E-02 263.9 0.12

```

SPECTRAL RADIANCE AND TRANSMITTANCE

WAVELTH (UM)	FREQ (CM**-1)	TRANS	TARG RAD (WATTS/M**2/SR/CM)	PATH RAD	TOTAL RAD	INSTR RESPONSE
3.8462	2600.000	0.8556	2.423E-05	4.050E-05	6.473E-05	0.0000
3.8035	2629.167	0.8552	2.369E-05	3.616E-05	5.984E-05	0.2083
3.7618	2658.333	0.8544	2.315E-05	3.237E-05	5.552E-05	0.4167
3.7209	2687.500	0.8535	2.262E-05	2.897E-05	5.160E-05	0.6250
3.6810	2716.667	0.8527	2.212E-05	2.592E-05	4.804E-05	0.8333
3.6419	2745.833	0.8519	2.163E-05	2.318E-05	4.481E-05	1.0000
3.6036	2775.000	0.8511	2.116E-05	2.071E-05	4.187E-05	1.0000
3.5661	2804.167	0.8503	2.070E-05	1.850E-05	3.921E-05	1.0000
3.5294	2833.333	0.8496	2.026E-05	1.652E-05	3.678E-05	1.0000
3.4934	2862.500	0.8488	1.983E-05	1.475E-05	3.458E-05	1.0000
3.4582	2891.667	0.8481	1.942E-05	1.316E-05	3.257E-05	1.0000
3.4237	2920.833	0.8474	1.902E-05	1.173E-05	3.075E-05	1.0000
3.3898	2950.000	0.8467	1.863E-05	1.046E-05	2.908E-05	1.0000
3.3566	2979.167	0.8460	1.825E-05	9.319E-06	2.757E-05	1.0000
3.3241	3008.333	0.8453	1.788E-05	8.300E-06	2.618E-05	1.0000
3.2922	3037.500	0.8447	1.753E-05	7.390E-06	2.492E-05	1.0000
3.2609	3066.667	0.8440	1.718E-05	6.578E-06	2.376E-05	1.0000
3.2301	3095.833	0.8434	1.685E-05	5.852E-06	2.270E-05	1.0000
3.2000	3125.000	0.8428	1.652E-05	5.205E-06	2.173E-05	1.0000
3.1704	3154.167	0.8422	1.621E-05	4.628E-06	2.083E-05	1.0000
3.1414	3183.333	0.8416	1.590E-05	4.113E-06	2.001E-05	0.8333
3.1128	3212.500	0.8410	1.560E-05	3.655E-06	1.926E-05	0.6250
3.0848	3241.667	0.8404	1.531E-05	3.246E-06	1.856E-05	0.4167
3.0573	3270.833	0.8399	1.503E-05	2.883E-06	1.791E-05	0.2083
3.0303	3300.000	0.8393	1.476E-05	2.559E-06	1.731E-05	0.0000

5.6 Example 6: A single wavelength scenario 3 calculation

The SCN3 card provides all parameters except wavelength/waveband for the scenario 3 imager. The angular resolution is 0.5 mr per pixel. A five column, three row array of radiance and temperature is stored after the parameter summary line in the data file (shown on the next page). The pixel size is large enough compared with the plume width that the values in the data array are area averaged. The -1 on the REFD card specifies a mean-value plume. The FGLW1.FDT file is shown on the next page.

```
INPUT:  REFD      90.000      2.000      3.      -1.
        SCEN     25.000 -1000.000    20.00    25.000    100.000    20.0
        SRCD      0.000      0.000      0.000
        METD      3.000    270.000    27.000    60.000    1009.728    4.000
        SCN3      0.50      5.      3.      0.
```

OUTPUT:

```
*****
*   EOSAEL 92   *
* 4D FITTE INPUT *
*****

FIRE TYPE: TRUCK

X-AXIS HEADING:    90.0 DEG CW FROM NORTH

POSITION M (      X      ,      Y      ,      Z      ) :
OBSERVER (      25.0, -1000.0,      20.0 )
TARGET   (      25.0,   100.0,      20.0 )
FIRE     (       0.0,       0.0,       0.0 )

METEOROLOGICAL DATA :
WINDSPEED      3.0 M/S      WIND DIRECTION    270.0 DEG
TEMPERATURE    27.0 C      RELATIVE HUMIDITY  60.0 %
AIR DENSITY    1009.7 G/M**3 PASQUILL CATEGORY 4

IMAGER DATA:
TOTAL FOV:    2.50 BY 1.50 (MR) RESOLUTION PER PIXEL 0.50 MR
PIXELS (HORIZONTAL, VERTICAL) ( 5, 3 )
WAVELENGTH 10.60 UM

PLUME CONSTANTS :
VERTICAL WIND (W0) 2.74 M/S COEFFICIENT (C) 7.530
BUOYANCY FLUX (F) 41.5 VIRTUAL SOURCE POSITION (M)
ENTRAINMENT CONSTANT 0.3820 XV: -6.17, ZV: -8.45

*****
* FGLW OUTPUT *
*****

AT 100. SECONDS AFTER START OF FIRE

RADIANCE AND TRANSMITTANCE DATA STORED FOR 5 COLUMN, 3 ROW ARRAY.
THE TOP LEFT CORNER PIXEL IS AT ( 24.00, 0.00, 20.50 ) M
AND THE ARRAY CENTER IS AT ( 25.00, 0.00, 20.00 ) M
IN A PLANE ( PERPENDICULAR TO THE LOS AND AT THE SOURCE DISTANCE
FROM THE OBSERVER ) IN THE USER COORDINATE SYSTEM.
POINT SPACING IS 0.500 M UNITS: Watts/m**2/sr/um

VALUES ARE AREA AVERAGED
```

The data file is listed below. The first row contains the following information:

- the (single or center-of-waveband) wavelength for the calculation,
- the number of columns and rows of imager data,
- the coordinates of the center of the upper left pixel in the plane of the fire,
- the angular resolution for one pixel,
- the coordinates of the center pixel in the array,
- the ambient temperature and
- a waveband function (used to convert waveband integrated radiance to a single-wavelength blackbody equivalent temperature).

The succeeding rows each contain (radiance and transmittance) data for one pixel.

10.60000	5	3	24.000	0.000	20.500	0.500	25.000	0.000	20.000	300.16	1.00
2.071363E+00	0.774										
2.438133E+00	0.738										
2.823721E+00	0.701										
3.216068E+00	0.666										
3.610541E+00	0.631										
2.705834E+00	0.713										
3.116120E+00	0.675										
3.534536E+00	0.638										
3.946305E+00	0.603										
4.343624E+00	0.571										
3.436608E+00	0.648										
3.874342E+00	0.611										
4.302427E+00	0.576										
4.709477E+00	0.544										
5.090297E+00	0.515										

5.7 Example 7: A scenario 3 waveband calculation

Note that for this example the calculation is done for a mean-value plume. The fourth parameter on the SCN3 'card' has been set to 1 to produce apparent temperature rather than radiance and transmittance output. The FGLOW1.FDT file is shown on the next page. See example 6 for a description of the information included in the file.

NOTE that this is no longer a recommended mode of operation. Unless apparent temperature information is the only information desired, it is more efficient to create a radiance and transmittance file and process it with the accessory programs described in Appendix A to obtain apparent temperature output.

```
INPUT:  REFD      90.000      2.000      3.      -1.
        SCEN     25.000 -1000.000  20.00    25.000   100.000   20.0
        SRCD      0.000      0.000      0.000
        METD      3.000    270.000    27.000    60.000  1009.728    4.000
        SCN3      0.50      5.      3.      1.
        BAND      1.      793.65   1162.79    15.      2.      0.

OUTPUT:

*****
*   EOSAEL 92   *
*  4D FITTE INPUT  *
*****

FIRE TYPE: TRUCK

X-AXIS HEADING:      90.0 DEG CW FROM NORTH

POSITION M (      X      ,      Y      ,      Z      ) :
OBSERVER (      25.0, -1000.0,      20.0 )
TARGET   (      25.0,      100.0,      20.0 )
FIRE     (      0.0,      0.0,      0.0 )

METEOROLOGICAL DATA :
WINDSPEED      3.0 M/S      WIND DIRECTION      270.0 DEG
TEMPERATURE     27.0 C      RELATIVE HUMIDITY    60.0 %
AIR DENSITY    1009.7 G/M**3  PASQUILL CATEGORY    4

IMAGER DATA:
TOTAL FOV:      2.50 BY      1.50 (MR)  RESOLUTION PER PIXEL 0.50 MR
PIXELS (HORIZONTAL, VERTICAL) (      5,      3 )
WAVEBAND FROM    793.65 CM-1 TO 1162.79 CM-1  CENTER WAVELENGTH 10.223 UM
15 POINTS RESOLUTION  INSTRUMENT RESPONSE: TRAP  MOLECULES INCLUDED: YES
APPARENT TEMPERATURE CALCULATED FOR CENTER WAVELENGTH

PLUME CONSTANTS :
VERTICAL WIND (W0)  2.74 M/S  COEFFICIENT (C)      7.530
BUOYANCY FLUX (F)  41.5      VIRTUAL SOURCE POSITION (M)
ENTRAINMENT CONSTANT 0.3820  XV: -6.17, ZV: -8.45

*****
* FGLOW OUTPUT *
*****

AT 100. SECONDS AFTER START OF FIRE

APPARENT TEMPERATURE DATA STORED FOR      5 COLUMN,      3 ROW ARRAY.
THE TOP LEFT CORNER PIXEL IS AT (      24.00,      0.00,      20.50 ) M
AND THE ARRAY CENTER IS AT      (      25.00,      0.00,      20.00 ) M
IN A PLANE ( PERPENDICULAR TO THE LOS AND AT THE SOURCE DISTANCE
FROM THE OBSERVER ) IN THE USER COORDINATE SYSTEM.
POINT SPACING IS      0.500 M      UNITS: degrees K

VALUES ARE AREA AVERAGED
```

The FGLOW1.FDT file is shown below.

10.22265	5	3	24.000	0.000	20.500	0.500	25.000	0.000	20.000	300.16	0.31
299.											
299.											
299.											
299.											
299.											
299.											
299.											
299.											
300.											
300.											
299.											
300.											
300.											
301.											
301.											

5.8 Example 8: A time-series of scenario 3 calculations at a single wavelength

The SCN3 and TCAL cards are used to create a sequence of images. The output data files, FLOW1.FDT, . . . , FLOW6.FDT, are not shown for this example. The output creates a series of files that span a five minute period and that are separated in time by one minute. Contour plots of the data are shown in Fig. 10. The accessory program XS2GRD was used to transform the data files to input files for the plotting program.

```

INPUT:  REFD      90.0      2.      3.      1.
        SCEN      5.0     -1000.0    6.0      5.0    100.0    6.0
        SRC      0.0      0.0      0.0
        METD      3.0     270.0    27.0      60.0   1009.728   4.0
        DETD      0.125
        TARG      10.0      0.8
        SCN3      0.125    121.      81.      0.
        TCAL      100.      60.      6.      0.

OUTPUT:

*****
*   EOSAEL 92   *
*  4D FITTE INPUT  *
*****

FIRE TYPE: TRUCK

X-AXIS HEADING:    90.0 DEG CW FROM NORTH

POSITION M ( X , Y , Z ) :
OBSERVER ( 5.0, -1000.0, 6.0 )
TARGET ( 5.0, 100.0, 6.0 )
FIRE ( 0.0, 0.0, 0.0 )

METEOROLOGICAL DATA :
WINDSPEED      3.0 M/S      WIND DIRECTION      270.0 DEG
TEMPERATURE     27.0 C      RELATIVE HUMIDITY    60.0 %
AIR DENSITY     1009.7 G/M**3  PASQUILL CATEGORY  4

IMAGER DATA:
TOTAL FOV:  15.13 BY 10.13 (MR)  RESOLUTION PER PIXEL 0.13 MR
PIXELS (HORIZONTAL, VERTICAL) ( 121, 81 )
WAVELENGTH 10.60 UM

PLUME CONSTANTS :
VERTICAL WIND (W0) 2.74 M/S  COEFFICIENT (C)      7.530
BUOYANCY FLUX (F)  41.5     VIRTUAL SOURCE POSITION (M)
ENTRAINMENT CONSTANT 0.3820  XV: -6.17, ZV: -8.45

*****
* FLOW OUTPUT *
*****

AT 100. SECONDS AFTER START OF FIRE

RADIANCE AND TRANSMITTANCE DATA STORED FOR 121 COLUMN, 81 ROW ARRAY.
THE TOP LEFT CORNER PIXEL IS AT ( -2.50, 0.00, 11.00 ) M
AND THE ARRAY CENTER IS AT ( 5.00, 0.00, 6.00 ) M
IN A PLANE ( PERPENDICULAR TO THE LOS AND AT THE SOURCE DISTANCE
FROM THE OBSERVER ) IN THE USER COORDINATE SYSTEM.
POINT SPACING IS 0.125 M UNITS: Watts/m**2/sr/um
THIS WAS REPEATED 6 TIMES AT 60 SECOND INTERVALS

```

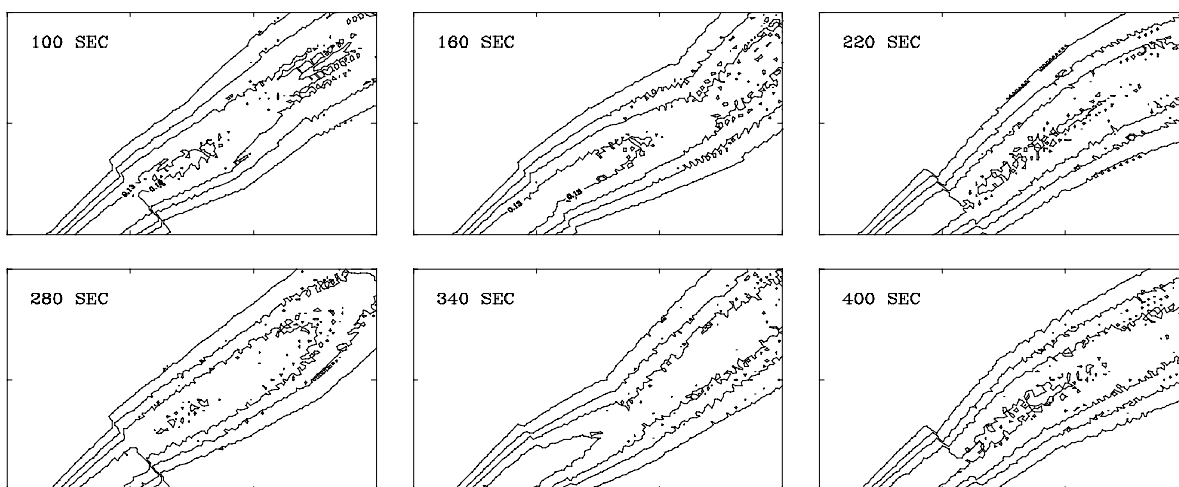


Figure 10a. Transmittance plots created with data from the example 8 simulation. Wavelength was $10.6\ \mu\text{m}$. Tic spacing is 5 m.

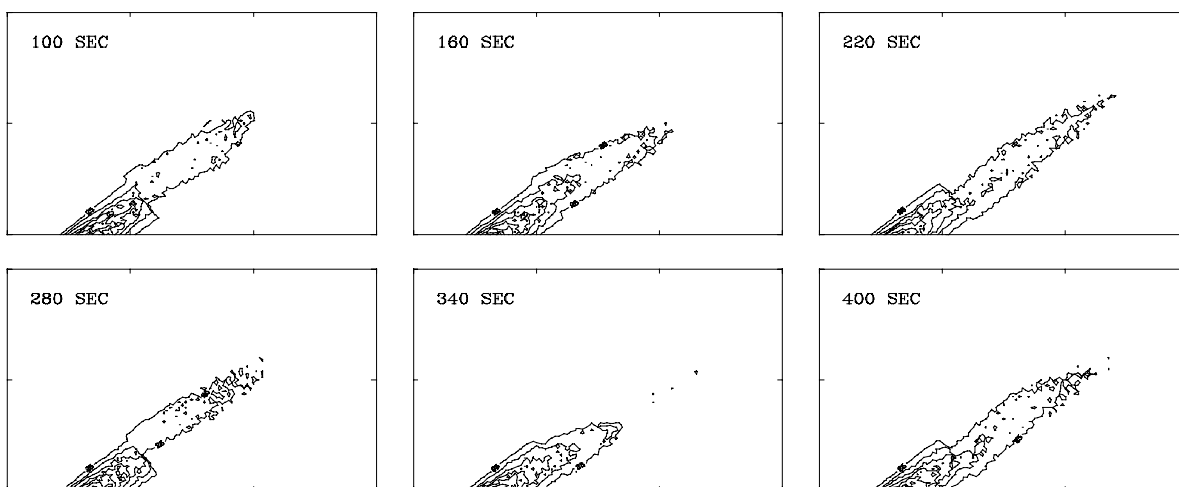


Figure 10b. Radiance plots created with data from the example 8 simulation. Wavelength was $10.6\ \mu\text{m}$. Tic spacing is 5 m.

5.9 Example 9: Internal cycling with variation of wind direction to produce 5 output files.

Use of the GO and DONE cards to perform a series of calculations with variation of parameters other than time is illustrated here. The five pages of the EX9.OUT file are shown. Figure 11 was prepared from the five (FGLOWn.FDT) data files. The accessory program XS2GRD was used to transform the data files to produce apparent temperature output files for the plotting program.

```

INPUT:  REFD      90.000      2.000      3.      1.
        SCEN      5.000 -1000.000      5.00      5.000      100.000      5.0
        SRCD      0.000      0.000      0.000
        METD      3.000      330.000      27.000      60.000      1009.728      4.000
        SCN3      0.125      121.      81.      0.
        GO
        METD      3.000      300.000      27.000      60.000      1009.728      4.000
        GO
        METD      3.000      270.000      27.000      60.000      1009.728      4.000
        GO
        METD      3.000      240.000      27.000      60.000      1009.728      4.000
        GO
        METD      3.000      210.000      27.000      60.000      1009.728      4.000
        DONE

```

OUTPUT:

```

*****
*   EOSAEL 92   *
* 4D FITTE INPUT *
*****

FIRE TYPE: TRUCK

X-AXIS HEADING:      90.0 DEG CW FROM NORTH

POSITION M (      X      ,      Y      ,      Z      ) :
OBSERVER (      5.0, -1000.0,      5.0 )
TARGET   (      5.0,   100.0,      5.0 )
FIRE     (      0.0,      0.0,      0.0 )

METEOROLOGICAL DATA :
WINDSPEED      3.0 M/S      WIND DIRECTION      330.0 DEG
TEMPERATURE     27.0 C      RELATIVE HUMIDITY     60.0 %
AIR DENSITY    1009.7 G/M**3      PASQUILL CATEGORY      4

IMAGER DATA:
TOTAL FOV:  15.13 BY  10.13 (MR)      RESOLUTION PER PIXEL 0.13 MR
PIXELS (HORIZONTAL, VERTICAL) ( 121,  81 )
WAVELENGTH      3.60 UM

PLUME CONSTANTS :
VERTICAL WIND (W0)      2.74 M/S      COEFFICIENT (C)      7.530
BUOYANCY FLUX (F)      41.5      VIRTUAL SOURCE POSITION (M)
ENTRAINMENT CONSTANT    0.3820      XV:   -6.17,  ZV:   -8.45

*****
* FGLOW OUTPUT *
*****

AT 100. SECONDS AFTER START OF FIRE

RADIANCE AND TRANSMITTANCE DATA STORED FOR 121 COLUMN,  81 ROW ARRAY.
THE TOP LEFT CORNER PIXEL IS AT (      -2.50,      0.00,      10.00 ) M
AND THE ARRAY CENTER IS AT      (      5.00,      0.00,      5.00 ) M
IN A PLANE ( PERPENDICULAR TO THE LOS AND AT THE SOURCE DISTANCE
FROM THE OBSERVER ) IN THE USER COORDINATE SYSTEM.
POINT SPACING IS      0.125 M      UNITS: Watts/m**2/sr/um

```

```

*****
*   EOSAEL 92   *
* 4D FITTE INPUT *
*****

FIRE TYPE: TRUCK

X-AXIS HEADING:      90.0 DEG CW FROM NORTH

POSITION M ( X , Y , Z ) :
OBSERVER ( 5.0, -1000.0, 5.0 )
TARGET ( 5.0, 100.0, 5.0 )
FIRE ( 0.0, 0.0, 0.0 )

METEOROLOGICAL DATA :
WINDSPEED      3.0 M/S      WIND DIRECTION      300.0 DEG
TEMPERATURE    27.0 C      RELATIVE HUMIDITY    60.0 %
AIR DENSITY    1009.7 G/M**3      PASQUILL CATEGORY    4

IMAGER DATA:
TOTAL FOV: 15.13 BY 10.13 (MR)      RESOLUTION PER PIXEL 0.13 MR
PIXELS (HORIZONTAL, VERTICAL) ( 121, 81 )
WAVELENGTH      3.60 UM

PLUME CONSTANTS :
VERTICAL WIND (W0) 2.74 M/S      COEFFICIENT (C)      7.530
BUOYANCY FLUX (F) 41.5      VIRTUAL SOURCE POSITION (M)
ENTRAINMENT CONSTANT 0.3820      XV: -6.17, ZV: -8.45

*****
* FGLow OUTPUT *
*****

AT 100. SECONDS AFTER START OF FIRE

RADIANCE AND TRANSMITTANCE DATA STORED FOR 121 COLUMN, 81 ROW ARRAY.
THE TOP LEFT CORNER PIXEL IS AT ( -2.50, 0.00, 10.00 ) M
AND THE ARRAY CENTER IS AT ( 5.00, 0.00, 5.00 ) M
IN A PLANE ( PERPENDICULAR TO THE LOS AND AT THE SOURCE DISTANCE
FROM THE OBSERVER ) IN THE USER COORDINATE SYSTEM.
POINT SPACING IS 0.125 M      UNITS: Watts/m**2/sr/um

```

```

*****
*   EOSAEL 92   *
*  4D FITTE INPUT  *
*****

FIRE TYPE: TRUCK

X-AXIS HEADING:      90.0 DEG CW FROM NORTH

POSITION M ( X , Y , Z ) :
OBSERVER ( 5.0, -1000.0, 5.0 )
TARGET ( 5.0, 100.0, 5.0 )
FIRE ( 0.0, 0.0, 0.0 )

METEOROLOGICAL DATA :
WINDSPEED      3.0 M/S      WIND DIRECTION      270.0 DEG
TEMPERATURE     27.0 C      RELATIVE HUMIDITY     60.0 %
AIR DENSITY    1009.7 G/M**3  PASQUILL CATEGORY 4

IMAGER DATA:
TOTAL FOV: 15.13 BY 10.13 (MR) RESOLUTION PER PIXEL 0.13 MR
PIXELS (HORIZONTAL, VERTICAL) ( 121, 81 )
WAVELENGTH      3.60 UM

PLUME CONSTANTS :
VERTICAL WIND (W0) 2.74 M/S COEFFICIENT (C) 7.530
BUOYANCY FLUX (F) 41.5 VIRTUAL SOURCE POSITION (M)
ENTRAINMENT CONSTANT 0.3820 XV: -6.17, ZV: -8.45

*****
* FGLOW OUTPUT *
*****

AT 100. SECONDS AFTER START OF FIRE

RADIANCE AND TRANSMITTANCE DATA STORED FOR 121 COLUMN, 81 ROW ARRAY.
THE TOP LEFT CORNER PIXEL IS AT ( -2.50, 0.00, 10.00 ) M
AND THE ARRAY CENTER IS AT ( 5.00, 0.00, 5.00 ) M
IN A PLANE ( PERPENDICULAR TO THE LOS AND AT THE SOURCE DISTANCE
FROM THE OBSERVER ) IN THE USER COORDINATE SYSTEM.
POINT SPACING IS 0.125 M UNITS: Watts/m**2/sr/um

```

```

*****
*   EOSAEL 92   *
* 4D FITTE INPUT *
*****

FIRE TYPE: TRUCK

X-AXIS HEADING:      90.0 DEG CW FROM NORTH

POSITION M ( X , Y , Z ) :
OBSERVER ( 5.0, -1000.0, 5.0 )
TARGET ( 5.0, 100.0, 5.0 )
FIRE ( 0.0, 0.0, 0.0 )

METEOROLOGICAL DATA :
WINDSPEED      3.0 M/S      WIND DIRECTION      240.0 DEG
TEMPERATURE    27.0 C      RELATIVE HUMIDITY    60.0 %
AIR DENSITY    1009.7 G/M**3      PASQUILL CATEGORY    4

IMAGER DATA:
TOTAL FOV: 15.13 BY 10.13 (MR)      RESOLUTION PER PIXEL 0.13 MR
PIXELS (HORIZONTAL, VERTICAL) ( 121, 81 )
WAVELENGTH      3.60 UM

PLUME CONSTANTS :
VERTICAL WIND (W0) 2.74 M/S      COEFFICIENT (C)      7.530
BUOYANCY FLUX (F) 41.5      VIRTUAL SOURCE POSITION (M)
ENTRAINMENT CONSTANT 0.3820      XV: -6.17, ZV: -8.45

*****
* FGLow OUTPUT *
*****

AT 100. SECONDS AFTER START OF FIRE

RADIANCE AND TRANSMITTANCE DATA STORED FOR 121 COLUMN, 81 ROW ARRAY.
THE TOP LEFT CORNER PIXEL IS AT ( -2.50, 0.00, 10.00 ) M
AND THE ARRAY CENTER IS AT ( 5.00, 0.00, 5.00 ) M
IN A PLANE ( PERPENDICULAR TO THE LOS AND AT THE SOURCE DISTANCE
FROM THE OBSERVER ) IN THE USER COORDINATE SYSTEM.
POINT SPACING IS 0.125 M      UNITS: Watts/m**2/sr/um

```

```

*****
*   EOSAEL 92   *
* 4D FITTE INPUT *
*****

FIRE TYPE: TRUCK

X-AXIS HEADING:      90.0 DEG CW FROM NORTH

POSITION M ( X , Y , Z ) :
OBSERVER ( 5.0, -1000.0, 5.0 )
TARGET ( 5.0, 100.0, 5.0 )
FIRE ( 0.0, 0.0, 0.0 )

METEOROLOGICAL DATA :
WINDSPEED      3.0 M/S      WIND DIRECTION      210.0 DEG
TEMPERATURE    27.0 C      RELATIVE HUMIDITY    60.0 %
AIR DENSITY    1009.7 G/M**3      PASQUILL CATEGORY    4

IMAGER DATA:
TOTAL FOV: 15.13 BY 10.13 (MR)      RESOLUTION PER PIXEL 0.13 MR
PIXELS (HORIZONTAL, VERTICAL) ( 121, 81 )
WAVELENGTH      3.60 UM

PLUME CONSTANTS :
VERTICAL WIND (W0) 2.74 M/S      COEFFICIENT (C)      7.530
BUOYANCY FLUX (F) 41.5      VIRTUAL SOURCE POSITION (M)
ENTRAINMENT CONSTANT 0.3820      XV: -6.17, ZV: -8.45

*****
* FGLow OUTPUT *
*****

AT 100. SECONDS AFTER START OF FIRE

RADIANCE AND TRANSMITTANCE DATA STORED FOR 121 COLUMN, 81 ROW ARRAY.
THE TOP LEFT CORNER PIXEL IS AT ( -2.50, 0.00, 10.00 ) M
AND THE ARRAY CENTER IS AT ( 5.00, 0.00, 5.00 ) M
IN A PLANE ( PERPENDICULAR TO THE LOS AND AT THE SOURCE DISTANCE
FROM THE OBSERVER ) IN THE USER COORDINATE SYSTEM.
POINT SPACING IS 0.125 M      UNITS: Watts/m**2/sr/um

```

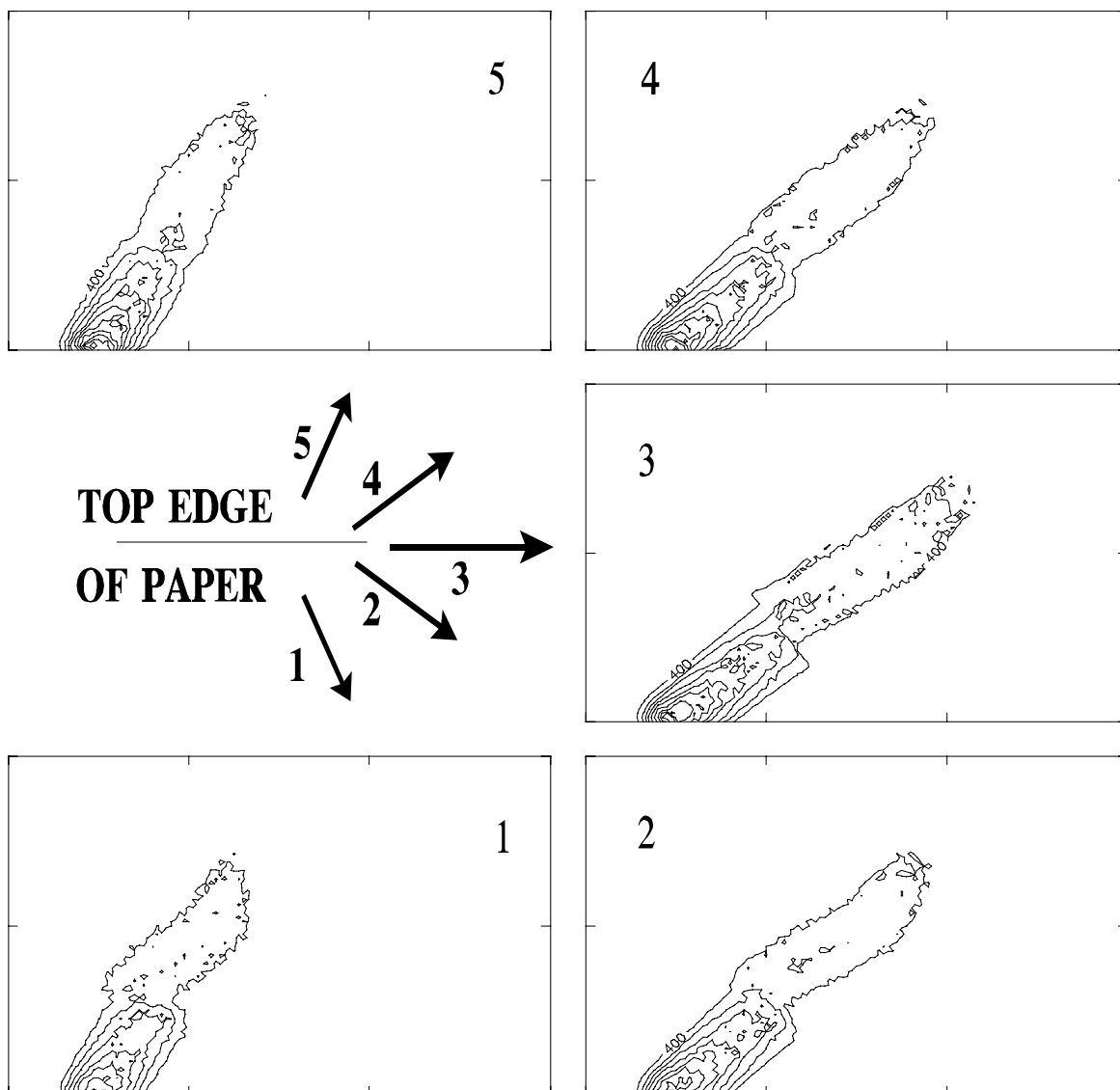


Figure 11. Apparent temperature plots for various wind directions indicated. Prepared from the data files of the example 9 simulation. Wavelength was $3.6 \mu\text{m}$.

Acknowledgment

The author wishes to acknowledge helpful discussions at the start of this work with Dr. Donald Walters and Dr. Kenneth Kunkel about atmospheric turbulence theory and measurements, and recent discussions with Dr. Donald Hooch about fractal representations of fluctuational quantities. She is also indebted to Dr. Charles Bruce for data and discussions of its interpretation and to Wendell Watkins and his co-workers for transmittance and calibrated imagery data. Members of the NATO Research Study Group 15 and their technical support associates provided many interesting discussions and extensive data that were useful in model evaluation. Special thanks are extended to Dr. Dieter Clement of the Forschungsinstitut für Optik for arranging to share the model enhancements that they supported.

References

- Briggs, G. A., 1969, Plume Rise, U.S. Atomic Energy Commission, TID-25075, Oak Ridge, TN
- Bruce, C. W., and N. M. Richardson, 1983, 'Propagation at 10 μm through smoke produced by atmospheric combustion of diesel fuel', Applied Optics, 22(7):1051-1055
- Bruce, C. W., S. B. Crow, Y. P. Yee, B. D. Hinds, D. Marlin, and A. V. Jelinek, 1989, 'Infra-Red Optical Properties of Diesel Smoke Plumes', Applied Optics, 28(19):4071-4076
- Bruce, C. W., T. F. Stromberg, K. P. Gurton and J. B. Mozer, 1991, 'Trans-spectral absorption and scattering of electromagnetic radiation by diesel soot', Applied Optics, 30(12):1537-1546
- Bruce, D., 1987, Fire-Induced Transmission and Turbulence Effects Module FITTE, ASL-TR-0221-15, US Army Atmospheric Sciences Laboratory, White Sands Missile Range, NM 88002-5501
- Bruce, D., 1988, 'An Extended Emissive Source Simulation Model', Proceedings of the Society of Photo-Optical Instrumentation Engineers, Vol 926, SPIE, Bellingham, WA 98227-0010
- Bruce, D., 1989, 'A Comparison of Modelled Thermal Images of Fires with Field Test Data', Proceedings of the Smoke/Obscurants Symposium XIII, AMCPM-SMK-CT-001-89, OPM Smoke/Obscurants, Aberdeen Proving Ground, MD 21005
- Bruce, D., and R. A. Sutherland, 1986, 'FITTE Model Validation: A Status Report', Proceedings of the Sixth Annual EOSAEL/TWI Conference, US Army Atmospheric Sciences Laboratory, White Sands Missile Range, NM 88002-5501
- Bruce, D., R. A. Sutherland and D. Larson, 1982, 'Fire-Induced Transmission and Turbulence Effects Module FITTE', EOSAEL 82: Vol III, Transmission Through Battlefield Aerosols, ASL-TR-0122, US Army Atmospheric Sciences Laboratory, White Sands Missile Range, NM 88002-5501
- Fante, R. L., 1975, 'Electromagnetic Beam Propagation in Turbulent Media', Proc IEEE, 63(12):1669-1692
- Farmer, W. M., B. Locke, R. E. Davis and R. Laughman, 1989, U.S. Army Transmissometer Validation Program-Summary Report, STC Technical Report 3003, Science and Technology Corporation, 555 s. Telshor Blvd., Las Cruces, NM 88005
- George, W. K., R. L. Alpert, and F. Tamanini, 1977, 'Turbulence Measurements in an Axisymmetric Buoyant Plume', Int J Heat Mass Transfer, 20:1145-1154
- Gillespie, P. S., 1987, BEST-ONE Data Analysis and Comparison, OMI-237, OptiMetrics, Inc., 106 E. Idaho, Suite G, Las Cruces, NM 88005
- Gomez, R. B., R. A. Sutherland, L. S. Levitt and E. A. Olivas, 1980, "Products of Vehicle and Grass Fires Affecting Electro-Optical System Performance", Proceedings of the Society of Photo-Optical Instrumentation Engineers, Vol 219, Los Angeles Technical Symposium
- Hoult, D. P., J. A. Fay and L. J. Forney, 1969, 'A Theory of Plume Rise Compared with Field Observations', J. Air Pollut. Control Ass., 19:585-590

- Hoult, D. P. and J. C. Weil, 1972, 'A turbulent plume in a laminar crossflow', Atmos. Environ., 6:513-531
- Kaaijk, J., 1986, Chemical characterization of fire products, PML 1986-47, Prins Maurits Laboratorium, p o box 45, 2280 AA rijswijk, the Netherlands
- Kennedy, B. W., 1981, Battlefield Induced Contamination Test Project Summary, Internal Report, U.S. Army Atmospheric Sciences Laboratory, White Sands Missile Range, NM
- Kennedy, B. W., 1982, Battlefield Induced Contamination Test-III (BICT III), Internal Report, U.S. Army Atmospheric Sciences Laboratory, White Sands Missile Range, NM.
- Khanna, R., E. Burlbaw, and A. Deepak, 1982, Models for Macrophysical and Microphysical Properties of Fire Products, Final Report, Contract DAAG29-81-D-0100, U.S. Army Atmospheric Sciences Laboratory, White Sands Missile Range, NM
- Khanna, R. K., and H. L. Ammon, 1983, Optical Properties of Vehicular and Vegetative Fire Products, Technical Report 525, DAA629-81-D-0100, Battelle Columbus Laboratories, Columbus, OH
- Kneizys, F. X., E. P. Shettle, W. O. Gallery, J. H. Chetwynd, Jr., L. W. Abreu, J. E. A. Selby, S. A. Clough, and R. W. Fenn, 1983, Atmospheric Transmittance/Radiance: Computer Code LOWTRAN 6, AFGL-TR-83-0187, Air Force Geophysics Laboratory, Hanscom AFB, Bedford, MA
- Liedner, L., and D. Clement, 1987, 'Radiation Properties of Fires Derived from BEST ONE Data' in Proceedings of the Workshop on Measuring and Modelling the Battlefield Environment, North Atlantic Treaty Organization, Brussels, Belgium, 337-346
- Leslie, D. H., P. G. Eitner, J. L. Manning, and S. M. Singer, 1980, Infrared Electro-Optical System Performance Effects Due to Absorption by Battlefield Gases, ASL-CR-80-0127-2, U.S. Army Atmospheric Sciences Laboratory, White Sands Missile Range, New Mexico
- Levitt, B. W., and L. S. Levitt, 1982, 'Identification and Assessment of Factors Important in Modeling of Electro-Optical System Performance in Realistic Fire Situations', Optical Engineering, 21:148
- Manning, J. L., 1985, Addition of Molecular Transmittance and Radiance to Computer Code FITTE, OMI-136, OptiMetrics, Inc., 2000 Hogback Rd., Suite 3, Ann Arbor, MI.
- Manning, J. L., and K. A. Kebschull, 1988, The FFO 88 Version of the FITTE Code, OMI-292, OptiMetrics, Inc., 2008 Hogback Road, Suite 6, Ann Arbor, MI.
- Pinnick, R. G., G. Fernandez, B. D. Hinds, and P. Fishburn, 1982, Vehicular Dust and Fire Products Particle Size and Concentration Measurements in BIC-1 and BIC-2, Internal Report, U.S. Atmospheric Sciences Laboratory, White Sands Missile Range, NM, unpublished data
- Sutherland, R. A., and P. L. Walker, 1982, "Modelling Fire Products", Proceedings of Smoke Symposium VI, DRCPM-SMK-T-001-82, Harry Diamond Laboratories, Adelphi, MD
- Tatarski, V. I., 1971, The Effects of the Turbulent Atmosphere on Wave Propagation, U.S. Department of Commerce, Washington, DC
- Thompson, J. H., and J. G. DeVore, 1981, Analysis and Modelling of Battlefield Fire Plumes, ASL-CR-81-0072-2, U.S. Army Atmospheric Sciences Laboratory, White Sands Missile Range, NM

Turner, R. E., P. G. Eitner, and J. L. Manning, 1980, Analysis of Battlefield-Induced Contaminants for E-O SAEL, ASL-CR-80-0032, U.S. Army Atmospheric Sciences Laboratory, White Sands Missile Range, NM

Weil, J. C., 1981, 'Source Buoyancy Effects in Boundary Layer Diffusion', Proceedings of the Workshop on the Parameterization of Mixed Layer Diffusion, Physical Sciences Laboratory, New Mexico State University, Las Cruces, NM

Young, S. J., 1977, Description and Use of the Plume Radiation Code ATLES, SAMSO-TR-77-100, Aerospace Corporation, El Segundo, CA

Appendix A: Auxiliary Programs to Aid Visualization of FGLOW Output

Two accessory programs are provided to help with visualization of the image files created by FITTE. These programs are working examples that transform the FGLOWn.FDT files into forms that may be printed or imported into a graphics program that can produce contour plots. Both of the programs permit output of four quantities: radiance, transmittance, apparent (blackbody-equivalent) temperature and integrated path density (CL). The latter two quantities are obtained by transformation of the first two for the appropriate wavelength. (This would be the central wavelength for a waveband calculation.)

NOTE THAT SEPARATE SIMULATION RUNS ARE NO LONGER NECESSARY TO OBTAIN APPARENT TEMPERATURE IMAGES.

Recall that the FGLOWn.FDT output files should generally be renamed for storage since otherwise they will be overwritten the next time FITTE is run using the FGLOW identifier.

The programs have been written for use with equipment and software that we have on hand. This should not be construed as a recommendation or endorsement of the hardware and software.

Plots prepared with output from XS2GRD were shown in Chapter 5 with sample runs. A sample of output from XS2PRT is shown here.

A.1 XS2PRT

XS2PRT creates files containing greyscale printouts of the FGLOWn.FDT data. The files will have the same name as the input file with the extension FDT replaced by RAD, TRN, APT or DNS as appropriate. The example program is tailored for an HP Laserjet printer and uses control sequences and built-in fonts in creating the output files. The width of the image array (that is, the number of columns in the array) determines whether the output is printed in portrait or landscape mode or whether it is split into panels for printing.

If another printer will be used for these printouts it will be necessary to modify the program. This entails substitution of the appropriate printer control sequences (usually found in the printer manual) and modification of the numbers that determine when to split the output into panels. Fixed spacing fonts should be used and the number of characters per inch should be (nearly) equal to the number of lines per inch to give the image the correct proportions. The program is relatively well commented to assist in identifying areas where changes might be needed.

Figure A1 shows a printout of integrated path density that was created using this program. The simulation file used was the same file used to create the plume transmittance contour image shown in Fig. 4. The greyscale assignment table has been moved to the same page as the image for this example.

Figure A1. A pseudo-greyscale print of plume optical density produced with XS2PRT.

A.2 XS2GRD

XS2GRD is the program used to transform the FGLOWn.FDT files to a form that can be used by commercial software to create surface or contour plots. This program should be relatively easy to modify for use with other plotting packages. The format used for the output file is described in program comments.

Since the program I use for the contour plots expects a file extension of .GRD, the output files for this program have the extension .FDT replaced by R.GRD, T.GRD, A.GRD or D.GRD depending on which of the four types of data it contains.

Appendix B: Model Organization

Figure B1 shows the organization of FITTE. It can be called from EOSAEL main, or run as a standalone driver called by FITDRV.FOR. If FITDRV.FOR is used, it, along with its corresponding block data subroutine BLOCD.FOR, must be customized for the system on which it is to be run.

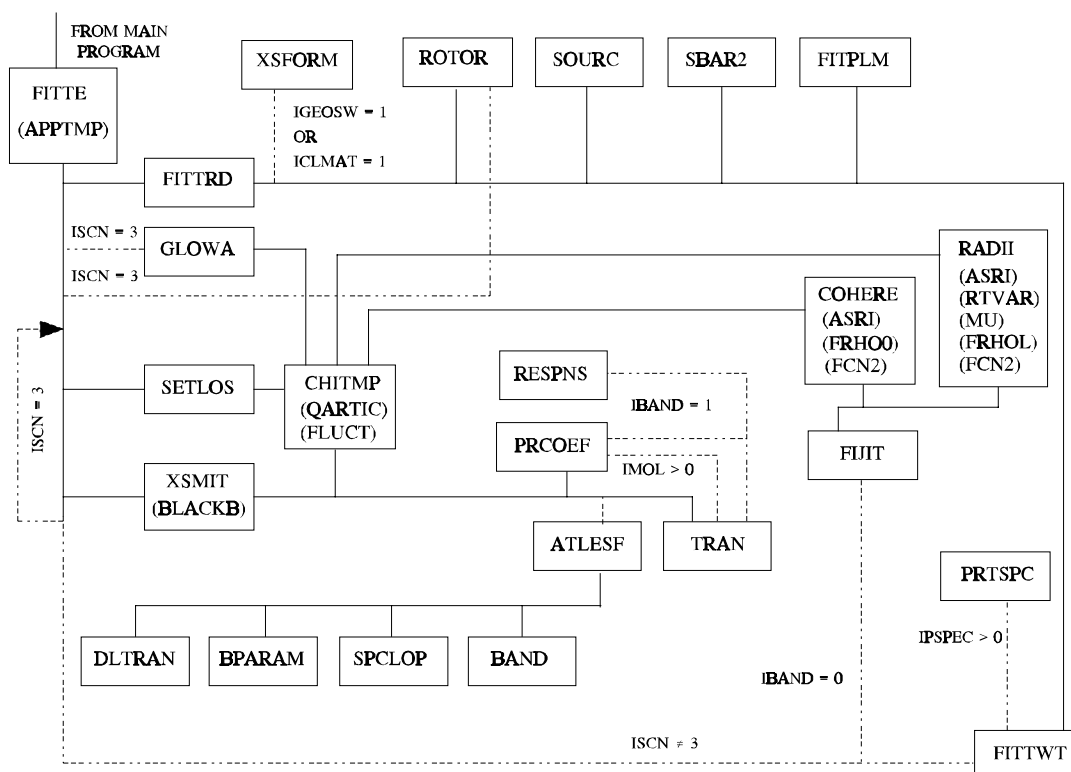


Figure B1. Diagram of FITTE model structure. Dashed lines indicate conditional calls. Functions, except EXPOF, listed in parentheses inside boxes.

In general, the subroutines called directly by FITTE are called once, except for XSMIT which is called once for each path segment. For Scenario 3, SETLOS is called to establish parameter values for each LOS of the image matrix.

The FITTE model consists of 26 subroutines and 12 functions. Either EOSAEL Main or FITDRV.FOR is used as the main program, and the corresponding block data routines, FITTBD or BLOCD respectively, must be linked with the program.

A brief description of each subroutine and function is given below. The subroutines are listed roughly as they are first called. Subroutines which perform specific related calculations are grouped together.

B.1 Subroutines

a. FITTE

FITTE is the subroutine which controls execution of the model. It calls subroutines to perform required calculations and to write model output files.

b. FITTRD

FITTRD controls reading of the FITTE input cards, checks the input values, substitutes defaults, if possible, when invalid data is encountered and calls subroutines to transform coordinates and units and to calculate plume constants for given input parameters.

b.1 XSFORM

XSFORM transforms EOSAEL common block input to units used by FITTE.

b.2 ROTOR

ROTOR performs transformation of coordinates to (and from) the wind-aligned system used by FITTE.

b.3 SOURC

SOURC sets values of fire parameters based on input from the REFD card and the SVAR card. Table 1 of this document shows the parameters for the various sources.

b.4 SBAR2

SBAR2 calculates the stability parameter needed to calculate the ambient lapse rate for FITTE. The routine is identical with subroutine SBAR1 used in the EOSAEL 82 version of model COMBIC.

b.6 FITPLM

FITPLM calculates the values of FITTE plume parameters.

c. GLOWA

GLOWA is called to calculate parameters needed for control of FGLOW (ISCN = 3) model execution.

d. CHITMP

CHITMP calculates values of plume distribution functions such as temperature and aerosol and molecular densities for a given point on the LOS.

d.1 FLUCT1

FLUCT1 calculates the displacement, due to wind fluctuations, of a plume centerline point from the mean centerline for the current calculation time.

d.2 FLUCT2

FLUCT2 calculates fluctuations in entrainment and combustion products due to wind fluctuations.

e. SETLOS

SETLOS calculates plume entry and exit points on the line of sight.

f. XSMIT

XSMIT controls calculation of the propagation parameters related to extinction and radiance. When molecular absorption effects are to be included ($IMOL > 0$) it calls the set of subroutines adapted from the ATLES model code.

g. ATLESF

ATLESF controls calculations of molecular absorption by the combustion products carbon dioxide and water vapor. Temperature dependent absorption coefficients are used for the calculations. Values are calculated for each of the NWVN wavenumbers if a waveband calculation is specified.

g.1 BAND

BAND reads the temperature dependent band model parameters.

g.2 SPCLOP

SPCLOP creates an array IWAVE to control the band model calculations.

g.3 BPARAM

BPARAM calculates band model parameters for a given wavenumber, path segment and specie of molecule.

g.4 DLTRAN

DLTRAN calculates the transmittance along a path segment for a single molecular specie.

h. TRAN

TRAN averages transmittances and integrates radiances over the waveband. It calls RESPNS to create an instrument response function array for use in these calculations and it calls PRCOEF to obtain the aerosol optical constants for each wavelength. For single wavelength calculations it transfers values from the calculation arrays to the output variables.

i. RESPNS

RESPNS calculates an array of instrument response coefficients for the wavenumbers used in a waveband calculation.

j. PRCOEF

PRCOEF assigns values of aerosol optical constants for a given wavelength.

k. FIJIT

FIJIT controls calculation of the optical turbulence effects parameters. It calls one or both of the routines listed below, depending on the FITTE scenario specified.

k.1 COHERE

COHERE calculates the lateral coherence length by using function ASRI to integrate the function FRHOO through the plume.

k.2 RADII

RADII performs the calculations described by Fante (1975), using ASRI to perform the necessary integrations. It assigns a value to ICASE to indicate which of the four calculation methods was used.

l. FITTWT

FITTWT controls formatting and printing of user input and model output. The output is tailored to the specified scenario. A warning is printed if defaults were substituted for any of the user specified variables and an error message is printed if fatal input data is detected. The value of MODE is used to specify whether input or output is written.

l.1 PRTSPC

PRTSPC prints a table of spectrally resolved transmittance and radiance data.

B.2 Functions

a. APPTMP

APPTMP is an inverse blackbody function that is used to produce apparent temperature output for FGLOW if the user sets IAPT = 1. For a waveband calculation, the evaluation is performed for the wavelength at the center of the band.

b. ASRI

ASRI is an adaptive Simpson's rule integration routine with a specified local error and a maximum permitted number of resolution increases. If the function being integrated does not meet the error tolerance after the maximum number of resolution increases for a given path interval, a flag is set to indicate that the integration error is greater than that specified.

c. BLACKB

BLACKB calculates the energy density of a blackbody of temperature T at wavelength λ .

d. EXPOF

EXPOF limits the allowed range of exponents to prevent program crashes due to calculation errors.

e. FCN2

FCN2 evaluates C_n^2 as a function of temperature at any point in the plume.

f. FLUCT3

FLUCT3 evaluates the local fractional fluctuation in plume temperature based on the assumption of a fractal spatial frequency distribution.

g. FLUCT4

FLUCT4 evaluates the local fractional fluctuation in plume effluents based on the assumption of a fractal spatial frequency distribution.

h. FRHO0

FRHO0 evaluates the integrand in the equation for RHO0 in subroutine COHER.

i. FRHOL

FRHOL evaluates the integrand in the equation for ρ_L in subroutine RADII.

j. MU

MU evaluates the ratio of short- to long- term averaged beam radius using numerical results (Fante, 1975). This function is used by subroutine RADII for case 2 calculations as described in the technical manual.

k. QARTIC

QARTIC solves a quartic equation to find the centerline point closest to a given LOS point. It is called by CHITMP.

l. RTVAR

RTVAR evaluates the variance of $1/T$ for function FCN2 of subroutine RADII. It uses a lookup table and an interpolation scheme.

Appendix C: Fluctuation Time-History Data Files

C.1 Basic Ideas Underlying the Fluctuation Data Files

Fire plumes move about in space as a function of time. The fluctuations of the centerline position at a given plume height are a result of fluctuations in the horizontal windspeed and wind direction since that plume segment was generated. The centerline fluctuations can be described by a deterministic model if the wind fluctuations are known. The fluctuations in temperature and effluent concentrations at any point in the plume are the result of turbulent mixing. For a simple fast-running model, the fluctuations can be approximated by a distribution with a turbulent power spectral density with amplitudes and phase angles based on random numbers. The amplitude fluctuations can be scaled using available data.

The minimum information needed to model a space- and time- varying (4D) plume is a set of random numbers and x- and y- wind fluctuation data.

Several additional considerations that are related to model simplicity were used in constructing the files.

- A time step of one second was defined for the calculations. The row number in the file corresponds to the number of seconds after the start of the fire. The data file must be long enough to describe plume transport after the fire burns out so a total file length of 2000 rows was chosen.
- It is desirable to be able to use the fluctuation data files for a range of windspeeds, so the wind fluctuation data should be normalized, that is, the data stored should be fractional fluctuations.
- Calculations of centerline displacement are based on the cumulative fluctuations since the displaced plume segment was created. These calculations are most easily and quickly performed if the wind fluctuation data is stored as cumulative fractional fluctuations.

If model performance is to be compared with data from field tests it is desirable to use a time-history file which reflects the wind conditions during the test. Construction of such a file is described below.

C.2 Construction of a Time-History File from Field Test Data

A time history file may be constructed from field test data if it meets the following criteria. The data must include windspeed and wind direction, it must be available at one second intervals, and it must contain (at least) 2000 observations.

The 2000 seconds worth of data must be averaged to obtain a mean windspeed and a mean wind direction. The mean windspeed and wind direction should be recorded for use as input on the METD input 'card'. The data must then be processed to obtain time histories of windspeed (a) in , and (b) perpendicular to, the mean wind direction.

The data can then be transformed and stored in a time-history file. This file, as mentioned earlier in the manual, must have three columns of data. The first column must contain a set of random numbers in the range -0.5 to 0.5, and with a mean of 0.00 ± 0.009 . The second column must contain the cumulative normalized fluctuations in the downwind component of the wind. If we define the mean windspeed to be U and the instantaneous windspeed in the mean wind direction to be u_i , the value in the n^{th} row of the second column is given by

$$\frac{1}{U} \sum_1^n (u_i - U). \quad (\text{c1})$$

The third column of the data file contains the cumulative normalized crosswind component. If we define the instantaneous value of the crosswind component to be v_i , the value in the n^{th} row of the third column is given by

$$\frac{1}{U} \sum_1^n v_i . \quad (\text{c2})$$

The time-history file is read with an unformatted READ statement that requires three values for each row, so the columnar values for each row should be separated by spaces or other separators recognized by FORTRAN.

Note: The existing file FIT4D.DAT should be renamed and the desired time-history file should be copied into FIT4D.DAT, since that is the filename used by FITTE for the time-history file.

Appendix D: Modification of Fire Parameters

The selection of fire parameters to provide realistic representations within the model is not a simple, straight forward process. There are also limitations, primarily imposed by model assumptions, which limit the fires that can be described. This appendix discusses these limitations, describes rough relations between model and physical fire parameters and suggests limits on parameter variation using the SVAR input card.

D.1 Model Limitations on Fire Parameters

FITTE was developed as a fast running code to model effects of small scale battlefield fires, and these were assumed to be vehicular fires. Table **D1** shows basic assumptions that were made, consistent with this objective, and associated model limitations. The first and second of these must be considered when fire parameters are varied. The size limits shown are approximate. It is difficult to set bounds for the heat output, but the values associated with the fires defined in the model are the right order of magnitude.

Table D1. Limitations Due to Model Assumptions

Model Assumption	Associated Limitations
1. The energy density of the fire plume is low compared with that of the atmosphere.	- Only small scale fires ($R < 10$ m) with low to moderate heat output can be handled.
2. The plume must have structural integrity.	- The fire has a minimum size ($R \geq 0.5$ m) and heat flux.
3. The mean plume centerline is described by a power law.	- Unusual windshear conditions cannot be handled. - Less accuracy under very low windspeed conditions
4. Fires are assumed to be circular	- Cannot easily be adapted to describe linear fires such as grass fires

The limits are intended to indicate that model predictions will have built-in unknown errors if parameters are varied to try to describe something like an oil well fire since that is a high energy density source.

The parameters that can be varied using the input card SVAR are the mean fire temperature, the aerosol efficiency factor, the fire radius and the burn time. It is possible to vary these parameters to examine the effect of uncertainties associated with their values or to provide a better comparison with field test data.

Variation of these parameters for the first purpose was discussed briefly in Chapter 4. For the second purpose, the following comments may be useful.

D.1.1 Developing Model Fire Parameters from Data

The burn time can be obtained from observation. The associated uncertainty lies in determining the end time for the fire. This should be chosen as the time when a cohesive plume ceases to exist.

The fire radius has a clear meaning for a pool fire in a circular tank. If another shape container is involved, such as a rectangular tank of dimensions $L \times W$ with $L < 2W$ an appropriate value would probably be $R = 0.5 (L + W)$. The exact shape is not critical, since the influx of air will modify the shape of the fire/fire plume so that it is quasi-circular.

The mean fire temperature can be estimated from a set of measurements above the fire. This can be tricky for a fire in the field and the estimate will have a relatively large uncertainty. The value used in the model was obtained as follows (use Kelvin temperatures):

1. The data was examined to obtain the (average of the) maximum observed temperature(s) for the thermocouples near the center of the fire. (The thermocouple array was at about the level of the flame tips.) This (average) value was assumed to be valid for a point at a radius of 1σ from the center of a Gaussian distribution. (The wind shifted the fire about and the thermocouple array was in an area with a narrow distribution function.)
2. The value was divided by $\exp(-.5)$ to obtain an estimate of the Gaussian maximum.
3. The ambient temperature was subtracted from the Gaussian maximum temperature to obtain the excess plume maximum temperature. That temperature was divided by 2.9 - the ratio of Gaussian/top hat distribution values for the observation conditions. The ambient temperature was then added to obtain the mean fire temperature.

It is extremely difficult to obtain a good measurement of the aerosol efficiency factor. The value built into FITTE should be appropriate under most conditions.

D.1.2 Checking Model Behavior When Varying Fire Parameters to Match Data

If plume image data (photographs, video or IR images) are available it is possible to check the plume behavior to ensure that the fire parameters used produce a realistic plume. The following checks may be made by comparing the data with information derived from the model output. The most accurate checks will be based on images taken from a crosswind position.

The quantities to be checked are the initial plume slope and the plume spread. A scenario 1 model run with the fire parameter variation will produce output that may be used to predict these values.

The ratio of the vertical wind to the windspeed gives the initial plume slope. The inverse tangent predicts the initial elevation angle. This should be compared with the slope or elevation angle obtained from the plume images. A short segment of the plume image should give the best value for this angle. (You may want to try this comparison with Example 10 to get an idea of the errors involved.)

The plume spread angle is the inverse tangent of the entrainment constant. This should be compared with the (full width) angular spread of the plume obtained from the image(s). Use as long a plume segment as possible for the most accurate result.

If agreement is good for both comparisons the model should provide good predictions of the propagation effects when the selected fire parameters are used. Good agreement for the initial elevation angle will depend on the

variability of the wind during the field test as well as the uncertainty in determining the angle from the images. The plume spread angle should agree within five degrees.

A scenario 3 run could also be used; then a printed simulated image could be produced with the accessory program XS2PRT and this could be compared directly with the real plume images.